MACQUARIE UNIVERSITY

Tracing shallow longitudinal preferential pathways of fluid movement using electrical geophysics

Masters of Research Thesis

Author: Anthony Finn (BSc) Macquarie University

Supervisor: Mark Lackie, Macquarie University

9/10/2017

Department of Earth and Planetary Sciences

Faculty of Science and Engineering

Macquarie University, North Ryde, Australia

Australian Society of Exploration Geophysicists

Table of Contents

Abstract

Assessment of gullies is essential in understanding the effects soil erosion has on resource management, urban planning, agricultural productivity and local environmental conditions. Commonly, prediction of gully head cut retreat has been disregarded due to the inherent complexities; this study proposes a method of analysing data to interpret potential pathways of Gully retreat. Through the implementation of electrical geophysics (Electrical Resistivity Imaging & Frequency Domain Electromagnetics) surveys positioned uphill of existing gullies shallow conductor's representative of Longitudinal preferential pathways (LPP) will be detected. ERI results detected conductors uphill of the head cut at varying distances showing resistivity values of 1-40 Ωm; these identified anomalous zones were confidently linked to form an LPP. Integrated geophysical datasets were generated allowing for interpreted traces of LPP to be drawn which are representative of the future pathway of head cut retreat. Through comparing currently existing gully assessment techniques it is suggested that a combination of geophysical prediction of LPP and LiDAR data is necessary for a complete understanding of existing gullies. Based on the results of this integration, informed and targeted management decisions can be developed to remediate current landforms and mitigate future gullying.

List of Figures

Statement of Originality

I declare that the work presented in this thesis is all the authors own work, except when otherwise acknowledged. The material presented has not been reproduced elsewhere, submitted to another university, or institution.

Printed Name:

Date:

Signature:

Acknowledgements

Firstly, I need to thank Macquarie University for the opportunity, facilities and ability to conduct my research. I then not only acknowledge but thank my supervisor Mark Lackie for all of his expertise, advice, knowledge, help and dry sense of humor (which I only got half the time). Without your field expertise, guidance and equipment this project would have been much harder than what it was. I hope the coming years are kind to you and that you eventually retire to that beach.

To Anthony Allwell and Chris Scott from the Tamworth Regional Council, thank you for all your help and assistance with access to the site. Both of you couldn't have been more obliging if you tried!

Thank you to my parents, Christopher and Christine Finn for supporting me through both years of the Masters to get me to this point. It wouldn't have been possible without everything you have done for me! To the rest of my family thank you for your care and support in keeping me sane throughout the year.

A special and odd acknowledgment goes to Carla Raymond and Mitchell Gerdes. You might never read this part but I can't begin to thank you for all the support you guys gave to me, without it I wouldn't have made it this far! There was a point in my Masters in which everything went wrong for me and I nearly dropped out; but you guys kept me going and so I wouldn't be here without you! I wish all the best for the both of you wherever you want to end up, just remember to take me with you for the Journey! They say friends are the family you choose, I would agree with that with all my heart although it is one strange family.

To Thusitha Bandara Nimalsiri, thank you for help keep me sane and for all the banter! Good luck with your PhD and I look forward to showing you more of Australia!

To Ruby Charlton Shick it may have not even been a year since we met but what a whirlwind it has been! I can't begin to thank you for all of your support, generosity and kindness from just talking it out with to reading my thesis! You deserve the very best that this world has to offer and I can't wait to be there when you get it!

As for the rest of the MQ crowd thanks for all your support and good vibes which helped me get through the year with my sanity still intact. I wish you all the best with your academic works and future ambitions.

Thank you to the Australian Society of Exploration Geophysicist for the generous scholarship towards my thesis.

Chapter 1: Introduction & Background

Understanding local hydrology and fluid migration patterns is crucial for effective and efficient management of agriculture practices, urban planning, erosion control, environmental conditions and existing infrastructure. Hydrology focuses on the movement of groundwater and surface run-off. Groundwater incorporates water infiltrating through the subsurface reaching a lower hydrological barrier and then moving laterally while surface run-off involves an excess in infiltration which results in water travelling over the surface (Zhou et al., 2001).

Recent research into the initiation and development of incision channels know as gullies has focused on erosion of consolidated and unconsolidated material caused by near surface groundwater (Beavis, 2000, Wu and Cheng, 2005). To effectively manage these erosional features through mitigation an understanding of the occurrence and future erosional pathways is required, although prediction is difficult when topographic variations are not obvious.

Local hydrological conditions will determine the nature of surface flows and groundwater movement including the infiltration depth, flow direction and rate of movement, although it is generally understood that water flows through physical or chemical channels known as ***preferential pathways*** (Clothier et al., 2007). Pathways develop within a medium due to the heterogeneities in the physical properties of the material that the water is flowing through.

Prediction and visualisation of preferential pathways is problematic as it would require witnessing real-time surface flows uphill from an existing gully to trace an expected pathway, which is neither feasible or economical (Valentin et al., 2005). It can be assumed that water flowing through a preferential pathway will saturate the soil leading to a higher electrical conductivity relative to the surrounding soil profiles (Clothier et al., 2007). If this is the case, then electrical geophysics has the potential to measure and detect these anomalous zones uphill of an existing gully feature. To this affect there is potential to trace these ***preferential pathways*** to predict the occurrence of physical channels prior to their erosional formation, specifically this study focuses on the prediction of Gully Head-cut Retreat (GHR).

1.1 Land degradation and erosion processes

Soil erosion is recognised as a significant issue globally (e.g. reference). Where the energy of overland flow exceeds the resistance of surface soil, erosion and net loss of material results. In time, this soil loss can produce an incised channel feature referred to as a gully, with the generally observed progress of gully development via head cut retreat depicted in Figure 1.

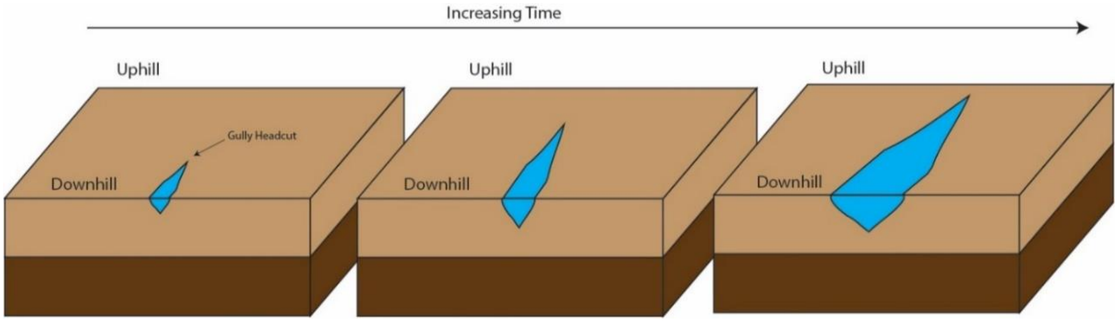

Figure 1. Visual representation of gully development over time. The blue area represents the current extent of gully erosion and over time (each block is a time slice) the gully is retreating uphill, this is referred to as '***head cut retreat***'.

1.1.1 Influences of Gully development

Initiation of gullying involves removal of sediment leading to small incision, continual erosion leads to gully head and wall instability resulting in the eventual channel development; which is depicted through Figure 1 seen as increasing dimensions of the blue area. Factors that determine the risk and rate of gullying processes the geological setting, soil type, soil strength, vegetation coverage, topographical features, slope, aspect and local climatic conditions (Shit and Maiti, 2012). Variations in geology will alter the development of gullies in the landscape as it relates to the resistance of the land to erosional processes (Corwin and Lesch, 2005b). Infiltration is determined by the topographical features and soil properties present in the area which includes the slope angle, aspect, terrain and soil profile; these variables will determine the kinetic energy produced by near surface groundwater which is directly proportional to the rate of gully erosion (Shit and Maiti, 2012). Local climate and weather conditions relate to the quantity and intensity of rainfall which is proportional to the amount of run-off produced, which is then relative to the rate of erosion (Vanmaercke et al., 2016).

Initiation of gullies has also been attributed to anthropogenic influences on land processes, mostly involving; inappropriate/intensive farming practices, vegetation clearing and urban development. These anthropogenic processes alter the local hydrological conditions changing the rainfall-runoff cycle, usually causing enhanced overland flows resulting in rapid sediment loss and eventual gullying (Stavi et al., 2010). All the processes, physical parameters and mathematical functions previously employed to assess gully formation and development aren't covered in this document but are covered in published literature seen as; Wilkinson et al. (2014), Stein and LaTray (2002) & Wells et al. (2009). The effects of anthropogenic processes on topographic conditions that effect gully development have also been detailed in Nazari Samani et al. (2009), Poesen et al. (2003) and Collison (2001).

Gullies can be differentiated into two categories based on the characteristics of the landform, these being; continuous and discontinuous (Le Roux and Sumner, 2012). Continuous gullies involve complete channels that fuse to a major stream or larger gully channel with no break/gap in the channel while discontinuous gullies involve an isolated scar in the landscape disconnected from other landform features (Beavis, 2000, Heede, 1982). Both types incorporate head-cuts but a discontinuous gully has an associated alluvial fan at the downhill end compared to the mouth of a continuous gully.

1.1.3 Head cut Retreat

Gully related studies have focused on lithology, topography, climate and anthropogenic factors that affect initiation and rate of erosion, although a critical feature of gullies is a dynamically retreating head-cut. It involves a dramatic increase in slope relative to the surrounding topography leading into the channel (Collison, 2001). Head cut retreat is the main form of uphill gully extension for continuous gullies but isn't a common focus or analytical feature in assessments of gully erosion. This form of erosion is driven by surface run-off concentrated towards the head-cut through preferential pathways resulting in the release of kinetic energy as water flows into the channel of the gully (Samani et al., 2016, Wells et al., 2009). Force exerted by concentrated flows results in intense erosional force leading to continual incision of the head-cut uphill extending the length of the existing gully (Stavi et al., 2010). The process of head cut retreat is continuous cycle of excess energy from overland flow incising into soil resulting in a material to break off into the channel which is then removed by channel flow. For a detailed outline and depiction of GHR refer to Collison (2001) and Stavi et al. (2010).

1.1.4 Consequences of soil erosion

Development of surface channel features result in significant damages to agricultural productivity, sustainable land management, environmental conditions and structural integrity of infrastructure (Beavis, 2000). Gullying is understood as one of the most detrimental and destructive forms of erosion for any agricultural industry as it involves; the removal of the top soil, reduction in soil fertility, destroying agricultural croplands, reduction in land/paddock connectivity and altering local hydrological conditions (Sidorchuk, 1999, Valentin et al., 2005). Removal of productive lands has severe economic consequences as reduction in productivity results in a net loss as well as the effort and finances required to mitigate further damage from gullying. Other major damages caused by gully extension is the undermining of existing infrastructure such as fences, buildings, roads and utilities (Perroy et al., 2010). Similarly, this poses significant economic loss through repairs for structural damage as well as costs associated with health risks from building failure (Frankl et al., 2012). Erosional features such as gullies pose significant risk and are extremely difficult to reverse so it is imperative to mitigate future erosion through timely and effective management based on confident prediction models.

1.2 Preferential Pathways – Water Residence

Local hydrology will determine the behaviour and movement of fluids over and through the subsurface while ultimately topographic variations controls the rate, location and extent of gully erosion (Zhou et al., 2001). It has been found in a study conducted by Melliger and Niemann (2010) that minor topographic changes will ultimately impact soil moisture patterns; specifically uphill of the gully head cut which varies in moisture relative to surrounding soils. As previously stated, the main driver for GHR is directed stream flow over the head-cut resulting in rapid erosion of unconsolidated material, this removal of sediment causes the head-cut to erode uphill over time (Clothier et al., 2007, Collison, 2001). Stream flows are generated by intense rainfall events which exceed the infiltration rate of the soil resulting in surface run-off. Water movement of these flows is controlled by the major and minor topographic variations of the area. Surface run-off will flow through preferential pathways created by minor topographic contours in the landscape otherwise known as preferential pathways of fluid migration.

1.2.1 Hydrological Model

Surface run-off on a broad scale is determined by major topographic contours although minor topographic variations within these govern localised flows resulting in feeding of water through preferential pathways, typically uphill of obvious features such as rivers and/or gullies (Frankl et al., 2012, Melliger and Niemann, 2010). Figure 2 represents a hydrology model in which surface run-off is focused to the lowest point (shown as purple arrows) as a preferential pathway, represented as the blue arrow, is developed due to the heterogeneities in the landscape represented as the red contour lines.

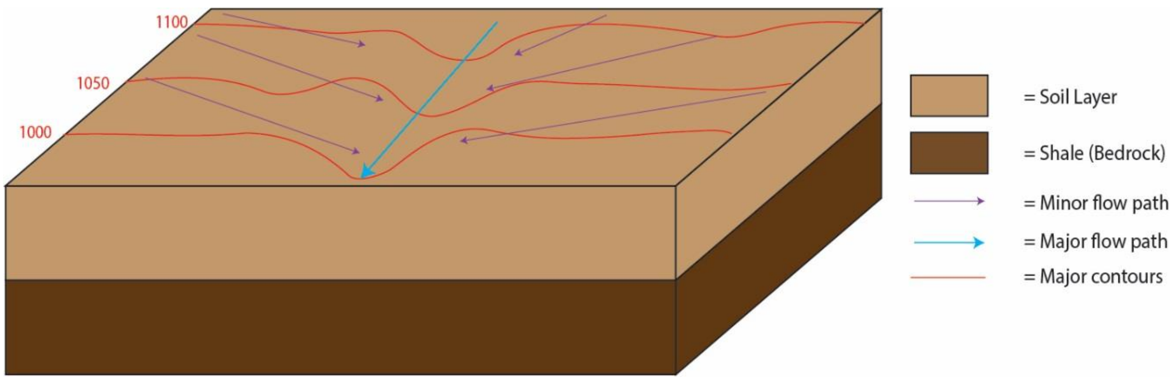

Figure 2. Model depicting the flow paths of water leading to a singular preferential pathway (blue arrow) caused by topographic variations in the surface Solid red lines represent major topographic contours which are indicative of a broad flow direction, Purple lines show minor flow paths.

As surface run-off is channelled as singular streams across a slope, the erosional force of water movement will eventually incise into the surface resulting in gullying. These preferential pathways represent the zone of the main body of water movement down a slope which can be inferred as a preferential pathway of water, which is represented as the blue arrow in Figure 2. Preferential pathways follow the dominate flow path of surface run-off from an uphill point to an existing surface feature, within this study these pathways are referred to as '***Longitudinal preferential pathways (LPP)***'.

1.2.2 Longitudinal Preferential Pathway

As LPP represent the dominate zones of water migration due to surface run-off from topographic highs to lows which is illustrated in Figure 2, this will inherently be associated with higher soil saturation percentages relative to the surrounding area. Zones of saturation occur due to higher quantities of water infiltration associated with LPP after a rainfall event. This leads to extended water retention in the soils associated with LPP relative to the surrounding soils.

Rainfall events produce heterogenous saturation of soils due to vegetation cover, soil type, soil depth and rainfall intensity, overall soils would experience fluctuations in apparent conductivity due to water content (Clothier et al., 2007). Preferential pathways represented as an LPP initially form on the soil surface as Figure 2 depicts as a 'Major Flow path' following the fluctuations of topography; this is then attributed to the heterogeneities in soil saturation. An LPP is associated with a larger quantity of water infiltration in the near-surface compared to the surrounding soils which would indicate that the soils within a LPP would be relatively more conductive. Differences within physical properties such as water content of soil can be exploited by geophysical investigations to identify variations in conductivity between LPP and topographically higher soils. Integrating geophysical surveying into hydrological studies provides an insight into the behaviour of fluid movement within the subsurface which is crucial to understanding LPP (Robinson et al., 2008).

1.3 Justification of Geophysical Methods

Existing literature, research and understanding on cost-effective and easy to implement prediction methods of gully erosion is minimal due to the complexities involved with this type of soil erosion (Valentin et al., 2005). Although factors which initiate and/or accelerate the rate of gullying are well understood as both environmental and anthropogenic; effective/accurate prediction of head-cut retreat doesn't currently exist. The main forms of gully assessment and prediction incorporates labour intensive field measurements such as; Global positioning satellite (GPS) which locates existing points within the channel, visual assessment (repeat photography), Light Detection and Ranging (LiDAR) and Photogrammetry (Perroy et al., 2010). These methods are implemented to quantify the spatial extent and sediment fluxes associated with gully erosion, due to the inability for Geographic Information Science to detect these small landform features. To a limited capacity results from such methods can be used to infer potential pathways for head-cut retreat with limited confidence/accuracy; this had led to the minimal research and predictive models into gully head-cut prediction being developed (Valentin et al., 2005).

To address this inability to predict GHR to allow for targeted management decisions to be developed alternative technologies to already known methods needs to be assessed. Geophysical investigations of physical properties of the earth has repeatedly proven its applicability and accuracy as a non-invasive technique for imaging of near surface and subsurface features (Zhou et al., 2001). Hydrological investigations incorporate analysis of water movement as surface run-off and infiltrated groundwater; characterisation of these is difficult as they cannot be observed directly. Integrating non-invasive geophysical techniques into hydrological assessments ("*hydrogeophyics*") allows for fluid migration patterns to be visualised and analysed in a spatial context (Robinson et al., 2008). Recent investigations have shown that integration of geophysics and hydrology (Corwin and Lesch, 2005b) results in a significant increase in site specific understanding of hydrological processes and interactions, which is required for assessment of LPP.

1.3.1 Geophysical Techniques

Assessment of LPP requires an adequate measuring and mapping of the variations in water content that exist across a soil profile associated with a slope. To measure these variations electrical geophysical investigations can be implemented to exploit the relative changes in resistivity/conductivity between saturated and unsaturated zones within the subsurface (Corwin and

Lesch, 2005a). The most commonly implemented electrical technique to measure the distribution of resistivity/conductivity of soils is '***Electrical Resistivity Imaging*** *(ERI)*'. It incorporates an analysis of the resistivity of the subsurface by measuring specific points at different depths within a profile (Robinson et al., 2008). Another common technique used is soil mapping is '***Frequency Domain Electromagnetics*** *(FEM)'* which induces electromagnetic currents within the near-surface (0-6m depth) to measure the bulk conductivity. These geophysical techniques are implemented within numerous industries to target shallow sub-surface variations in resistivity/conductivity based on heterogeneities of physical properties associated with the soil (Corwin and Lesch, 2005b).

Previous studies have implemented combinations of geophysical techniques including ERI and FEM for identification of near-surface features; these include an investigation on detecting cavities by Carrazza and Helene (2016) as well as another study into cave systems associated to urban hazards conducted by Lazzari et al. (2010). Carrazza and Helene (2016) conducted a near surface geophysical investigation implementing ERI for the detection of cavities. It was hypothesized that the piping phenomenon of soils generated these air-filled cavities related to material failure. Typically gully formations within their study area were caused by rapid material loss; leading to the cut back of the gully into the hillside. ERI profiles were conducted in close succession (5m line spacing) back from the edge of the zone of failure, gullies development was based on rapid large movements of material away from slope edge. It was found that cavities filled with air were detected as zones of high resistivity values (>15,000 Ωm) and were concluded to be associated with areas of slab failure. The study also detected large conductive anomalies ranging from 0-300 Ωm which were interpreted to be highly saturated soil/rock but were considered unrelated with gully formation for the study area. Lazzari et al. (2010) also implemented a near-surface geophysical investigation to detect cave systems using ERI and Ground Penetrating Radar. The aim of study was to develop a hazard map for the site as it was known for its subsurface cave systems which posed significant hazards to an urban context. Results of ERI found that cave systems were typically identified as zones of high resistivity exhibiting values of >1000 Ωm. Other observable features were large conductive anomalies that were interpreted as saturated zones of soil/rock exhibiting values of 1-60 Ωm.

1.4 Research Breakdown

1.4.1 Hypothesis

The hypothesis for this investigation is that shallow anomalous conductive features within a 1-40 Ωm range with no obvious topographic association will exist uphill from the head cuts of continuous gullies which are representative of an LPP zone.

1.4.2 Research Aims

The findings presented in this Master of Research thesis are intended to address the following research aims:

(1) Investigate the ability for electrical resistivity imaging and frequency electromagnetic field methods to detect shallow conductors uphill from existing gullies illustrative of higher water saturation

(2) Investigate the potential association between identified shallow conductors uphill from head cuts as a Longitudinal preferential pathway for water movement representative of a potential prediction method for Gully Head cut Retreat

1.4.3 Tasks Undertaken

Task to be undertaken to address the research aims stated previously include:

- Identification of appropriate gullies through satellite imagery (Geographic Information Science)
- Field observations through visual assessment and GPS positioning
- Geophysical surveys across the head-cut of the gully with subsequent surveys uphill from that location at various distances
- Data processing and identification of anomalous shallow conductive zones which can be associated and linked to the gully as LPP.
- Assessment of applicability and confidence in the field method through direct comparisons of current literature detailing other forms of gully assessment for effective management

Chapter 2: Site Overview

2.1 Site Overview

The area is located north of Tamworth city in NSW, west of the waste management facility and east of Moore Creek Road; depicted as the red outlined area of Figure 3. It is situated on the Tamworth Belt which lies within the New England fold belt located ~200km inland off the Eastern coast of NSW, Australia. The geology of the site is comprised of fluvial and marine sedimentary units, mainly involving limestones, shales, volcanoclastics, conglomerates and sandstones (Chappell, 1968). Within the site, the geology incorporates two major Paleozoic geological formations of the Tamworth belt, the first being the underlying Early-Mid Devonian ***Tamworth Group*** and the second the late Devonian ***Parry Group***.

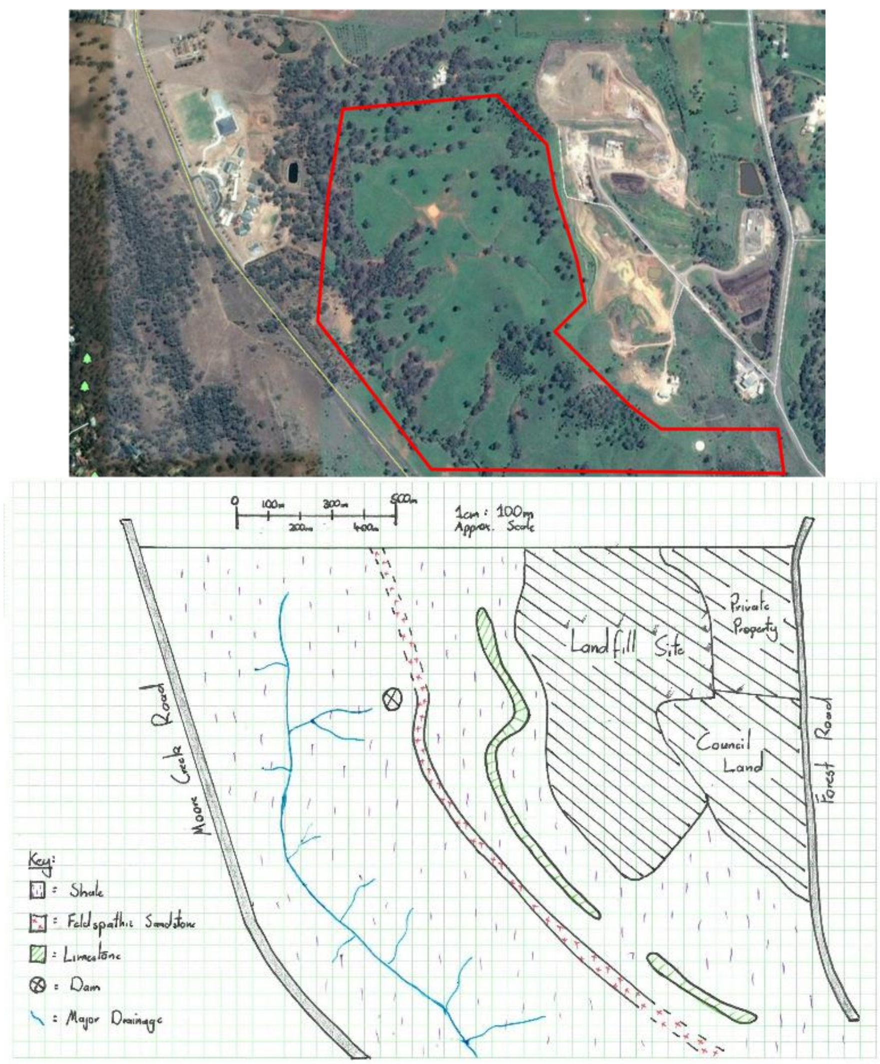

Figure 3. Depiction of the regional setting of the Tamworth site. Top Image: Google Earth image of site. Bottom Image: Localised geological map of the study area. Both images are located at 31°03'38.86" S 150°55'13.68" E and incorporate an approximate scale of 1cm:100m.

The Tamworth group consists of a sequence of sedimentary rocks including: conglomerate lenses, breccia's, cherts, limestones, volcaniclastics, feldspathic sandstones, siltstones and shales (Aitchison et al., 1992). Shales outcrop in the lower regions of the site as highly weathered surfaces with occasional lenses of the feldspathic sandstone, seen as the dominant geology of Figure 3. The Parry group outcrops as a series of semi-continuous limestone lenses which cap the hills in the central and eastern areas of the site, seen in Figure 3 as the limestone units. These lenses were deposited as Allochthonous bodies, carbonate reefs that have dropped off the shelf and settled in the sediments (Pohler, 1998).

Both groups have experienced low-grade metamorphism as well as major folding and faulting events, evident through the large-scale weathering of fault zones and small variations in regional bedding (Chappell, 1961). Measurements of regional bedding indicated a strike of 330-340^o and a general dip to the southwest of 35^o-45^o, variations are present within these units as they have been folded into upright open folds. Overall surface topography involves slope gradients of 10^o-25^o to the southwest (towards Moore Creek Road) and average soil profile depth of ~3m comprised of clay rich red gravels.

Chapter 3: Methods

Tracking of LPP and prediction of future gully extension uphill from existing features involves visual field assessment, as well as the implementation of electrical geophysics and the collection of accurate positional data. Fieldtrips to the 'Tamworth Waste Management facility' were conducted in Mid-February and then late April; timing of the fieldtrip affected the soil moisture of the area as the first fieldtrip involved extremely dry conditions compared to the second fieldtrip. Geophysical surveys were divided into primary and secondary sites labelled as sites A to E, these were determined based on the locations of existing gully features which are shown in Figure 4. Primary sites incorporated at least 4 ERI surveys, FEM and GPS positioning while secondary sites only involved 2 ERI surveys and GPS data. Differentiation of primary and secondary sites were determined by the development stage of present gullies as well as the ability to conduct surveys in the area. Targeted gullies matched the size of moderate to well-developed channels and represented similar formations as depicted in the centre and right models of Figure 1.

2.3 Geophysical Methods

2.3.1 Electrical Resistivity

Electrical resistivity surveys involved the use of 'Dipole-Dipole' electrode arrays with varying lengths of either a 100m (105 measurements) or 200m (257 measurements) having electrode spacings of 5m. Survey locations were based on the locations of known/located gully formations, shown as the solid red lines on Figure 4. Watering of electrodes occurred prior to measuring cycle to improve the contact. Measurements incorporated a maximum value of 'n'=7, so survey depth extended to approximately 15m. Equipment consisted of an 'ABEM Terrameter SAS 4000' for measurements and calculations of apparent resistivity and an 'ABEM LUND' to control current/potential electrode positions based on pre-set protocols; both connected to 12v batteries with a current input range of 20-200mA.

2.3.2 Frequency-Domain Electromagnetic (FEM)

Frequency Domain Electromagnetic surveys were conducted using a Dual EM system with a 4m Boom. Measurements were taken in the HCP mode every 2m along the survey line ensuring the centre of the boom was placed at the 2m interval, transmitter and receiver were kept North to South with the transmitter being more northerly. Approximate depth of penetration is ~4-6m and measures the bulk conductivity of the soil directly beneath the centre of the boom. Lengths of FEM surveys varied depending on the location of the survey and extent of the surface expression of the gully, Figure 4 depicts all FEM surveys as solid green lines.

2.4 GPS

To correlate geophysical data with gully positions, GPS data on the surface expressions of gullies was taken from the 'Head-cut' to a well-established point within the main channel. GPS information was collected using a combination of a 'Garmin E-trex' (2-5m accuracy) for approximate positions of survey lines and a 'Trimble R2' (1-2cm accuracy) for exact positioning of electrode locations, elevations and tracing channels of gullies shown as the solid yellow lines of Figure 4.

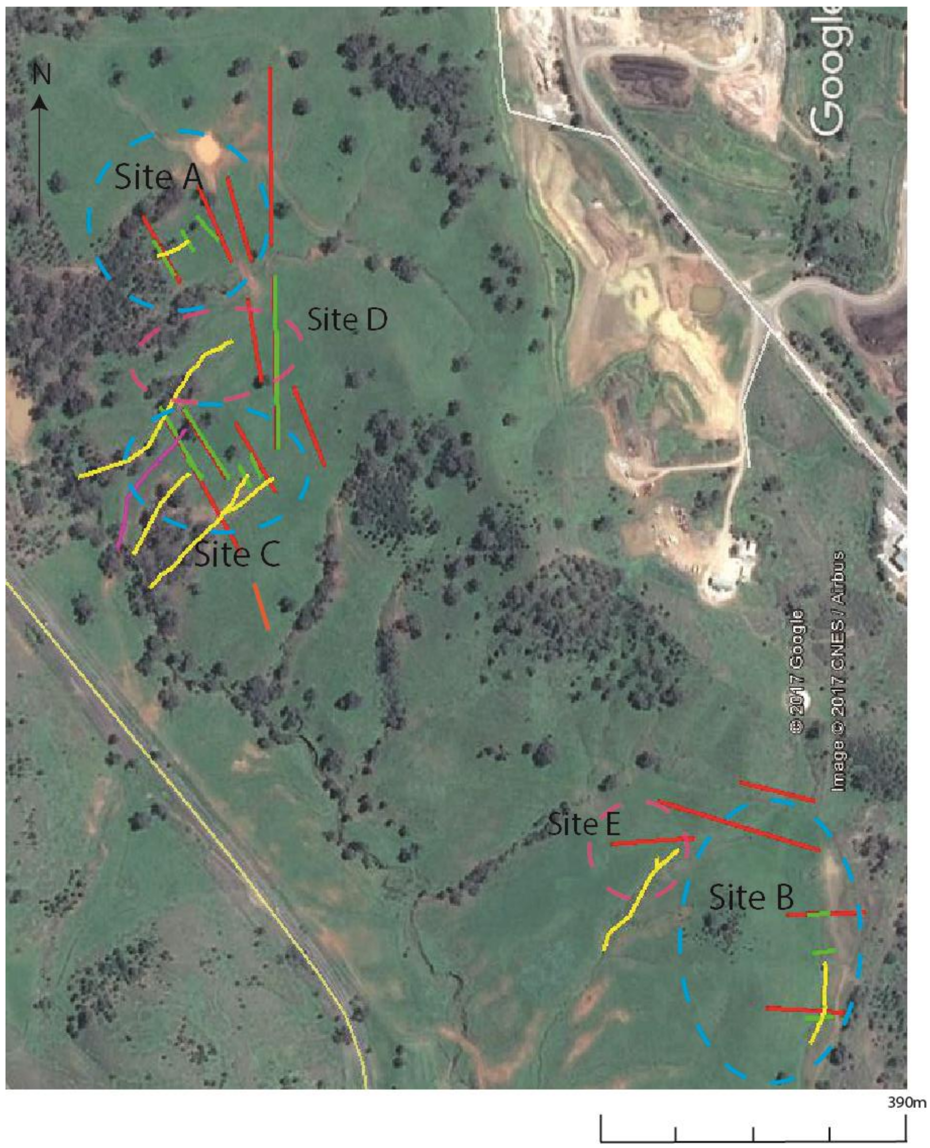

Figure 4. Image depicting the positions of all electrical resistivity (shown as solid red lines), FEM (shown as solid green lines) surveys and identified surface expressions of gullies (shown as solid yellow lines) across the site. Primary sites are represented by blue dashed circles and labelled as A, B, C. Secondary sites are depicted as pink dashed circles and labelled as D and E. Orange line depicts ERI survey conducted for background readings.

2.5 Data Processing & Filtering

Processing of resistivity data involved initial removal of data points from raw data files with a field calculated error of 10% and 5%, the percentage was determined based on the amount of data points collected. Edited data files were then imported and processed using 'Res2dinv' with a 'Robust Inversion Method' that incorporated an error change convergence limit of 0.1% and a maximum of 25 iterations. Further processing occurred after an inversion file was created in which the RMS error statistics were analysed and values over 100% were removed from the data file, data files were then re-processed with the same inversion technique to produce minimum error pseudo-sections of all resistivity lines. Additional information was included to each pseudo-section as topographic elevations for each electrode position. Acceptable error values were determined to be approximately 15-20%, this was an optimal range to preserve a significant amount of data points and achieving a minimum error. After filtering of errors has been completed profiles are then plotted with a logarithmic contour scale with a minimum value of 1-20 Ωm and a maximum value of 20,000 Ωm to produce final images. FEM processing involved generating scatter plots using excel for the Horizontal Coil and Vertical Coil components to visualize the variations in conductivities. The processing of FEM data involved taking multiple readings at the time of measurement.

Reasoning behind the large amount of filtering of the ERT data was due to the interference caused by nearby limestone features. Large anomalous resistivity readings of 20,000 Ωm and negative values were common in this area close to limestone outcrops resulting in datasets with data retention of 42% but as high as 98% away from the limestone.

Chapter 4: Results

The geophysical surveys are divided into primary and secondary sites; an image of these is given as Figure 4. Each site incorporates ERI and FEM surveys, the locations of which are given by a Google Earth image for each site. ERI results are shown as sections which depict variations in resistivity (Ωm) with location and depth. Resistivity surveys incorporate an approximate depth of 15m. Majority of surveys were conducted over a shale basement with a depth to basement of ~3-5m for each profile. Field and processing observations are included onto each profile as labelled/coloured boxes, along each profile if a representative box isn't present then it is considered alluvial material. FEM results are illustrated as line graphs which depicts both the Horizontal co-planar geometry (HC) and Perpendicular geometry (PC) values measured as milli-siemens per metre (mS/m).

4.1 Primary Sites

4.1.1 Site A

Site A incorporates four ERI surveys (ER1-4) and 3 FEM surveys (F1-3) over a gully in the North-West of the site, locations of the gully and geophysical surveys are depicted through Figure 5. The site incorporates a gently dipping slope to the South-West with mostly grass and sporadic tree ground coverage.

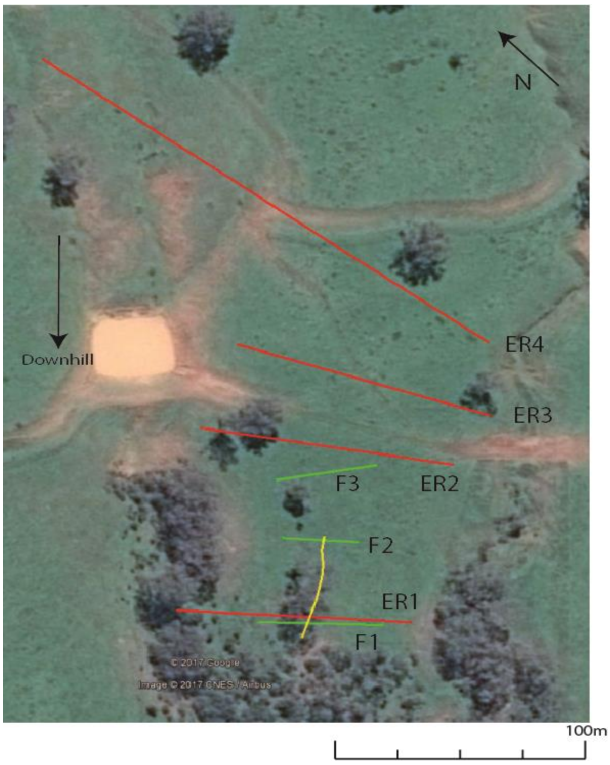

Figure 5. Google Earth image depicting the locations of ERI (Red lines) and FEM (Green Lines) surveys across an existing gully (Yellow line) for Site A. Surveys ER1, F1 and F2 were conducted over the gully while ER2 and F3 was 30m uphill, ER3 was 70m uphill and ER4 was 110m uphill of the head-cut.

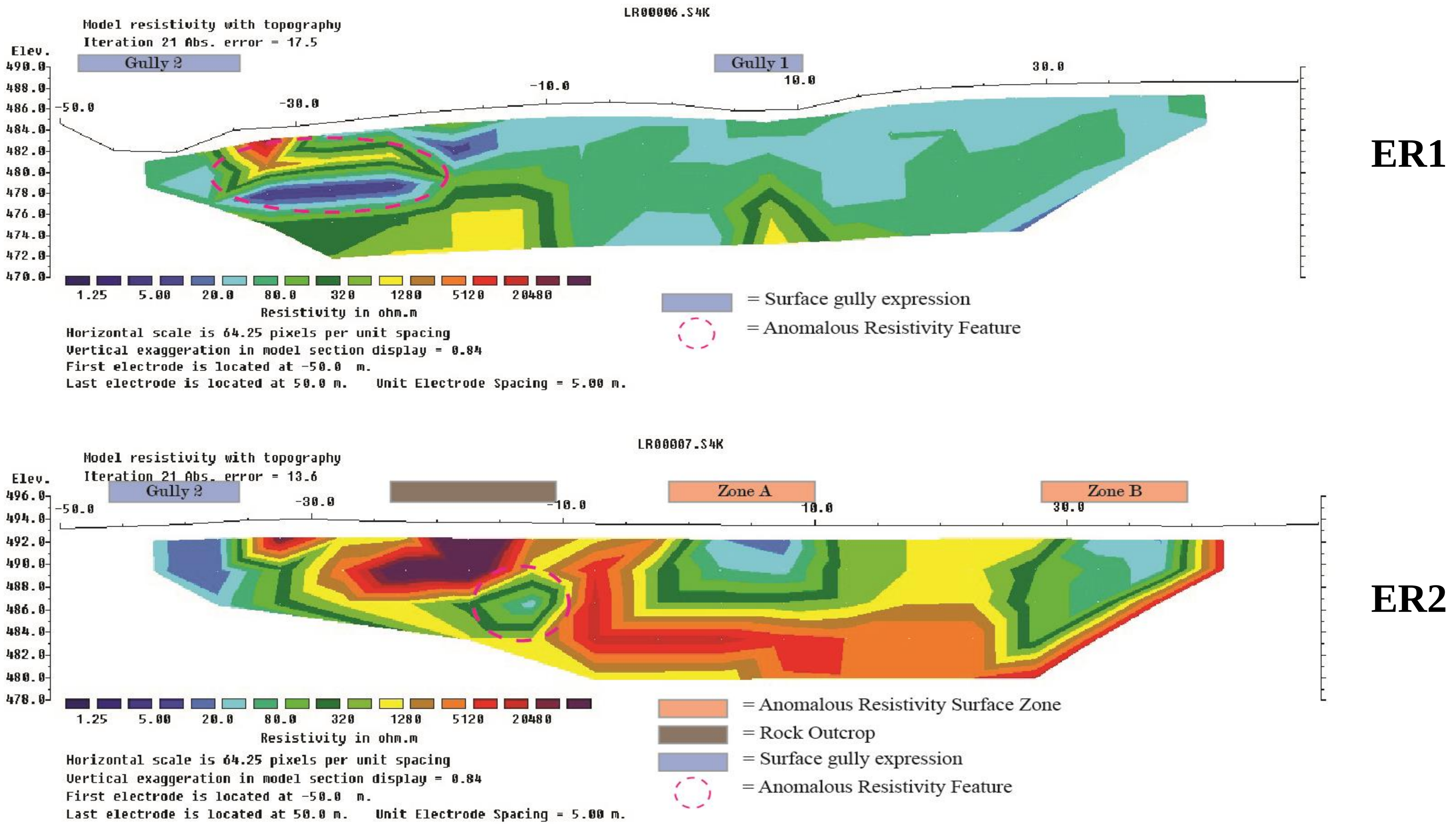

Figure 6a. Electrical Resistivity Imaging results for ER1 (Top) and ER2 (Bottom) for primary site A. Both profiles are 100m in length and incorporate the local topographic changes given via Trimble GPS system (2cm accuracy).

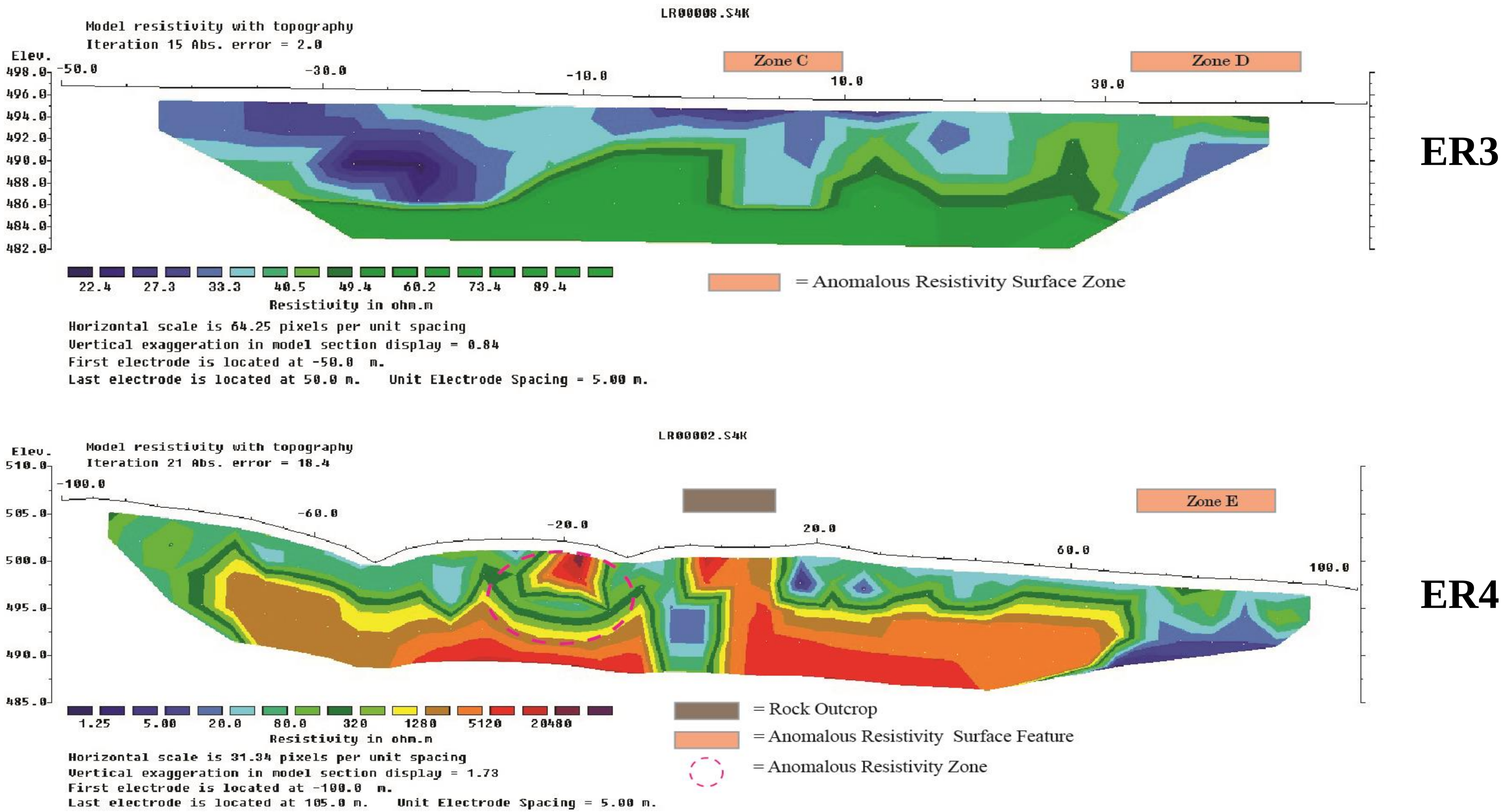

Figure 6b. Electrical Resistivity Imaging results for ER3 (Top) and ER4 (Bottom) for primary site A. ER3 is 100m in length and incorporates a different scale (1.25-90Ωm) relative to all other surveys; this is due to a different geological unit (Feldspathic Sandstone) being encountered resulting in a profile comprised of only soil. ER4 is 200m in length; both incorporate the local topographic changes given via Trimble GPS system (2cm accuracy).

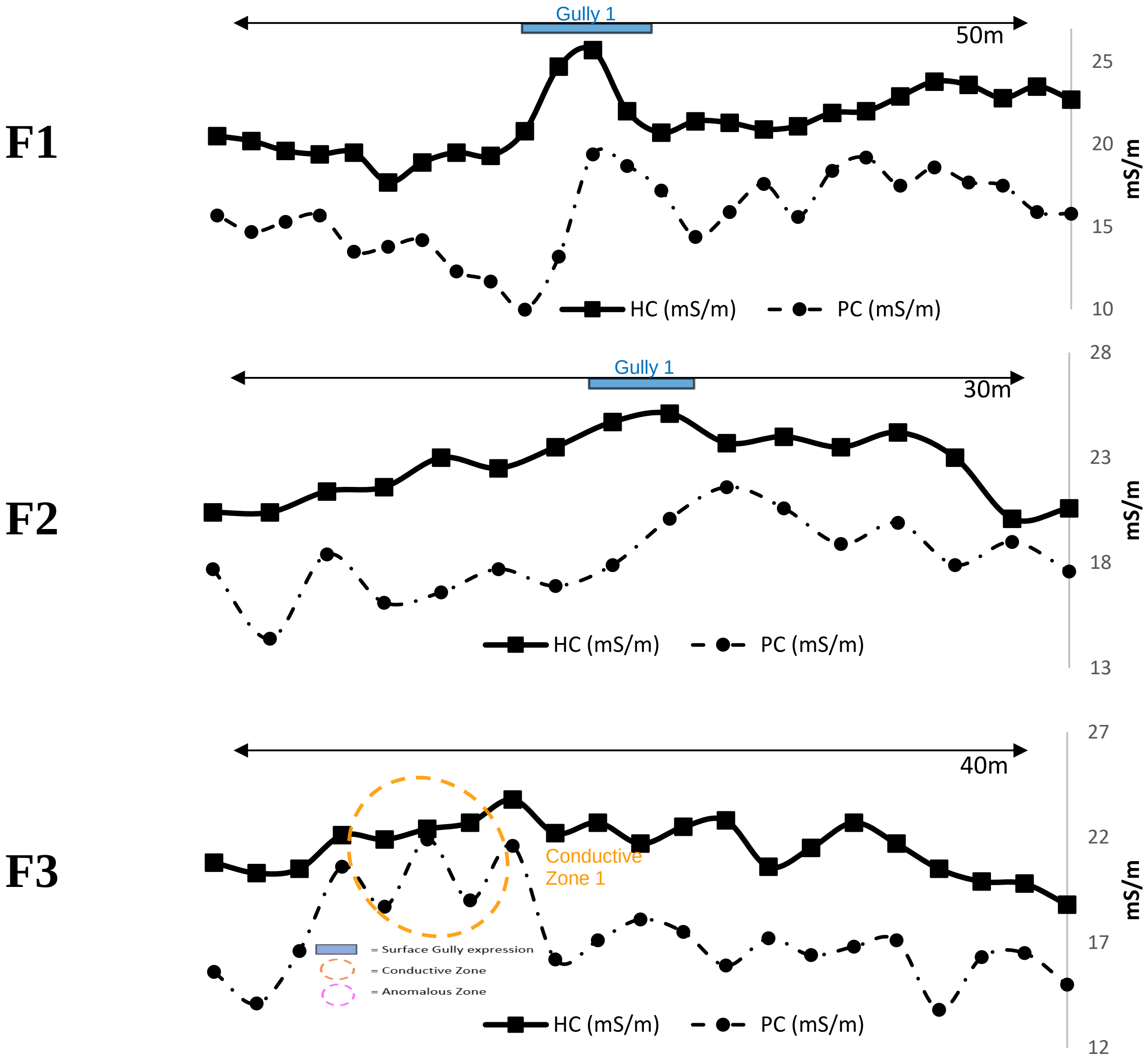

Figure 7. FEM results for profiles F1, F2 & F3 within site A. Vertical axis is in mS/m and the horizontal axis is in metres, distance between each data point is 2m. Obvious surface features that were encountered along survey lines are also illustrated

Figure 6a represents the ERI results for profiles ER1 and ER2. ER1 intersects two gully channels which are illustrated as "Gully 1" and "Gully 2" both depict minor relative changes in resistivity at 50-80 Ωm and show topographic changes in the profile. An anomalous zone is outlined by the dashed pink circle which depicts a resistor (5,000-10,000 Ωm) on the surface above a conductive zone (1-10. Majority of the profile exhibits low electrical resistivity comparatively to other surveys of 50-200 Ωm aside from 2 deeper resistors (1,000-5,000 Ωm) which represent the basement rock shown as the yellow features. ER2 intersects the continuation of "Gully 2" further uphill and depicts a more conductive zone than ER1 of 20 Ωm. An anomaly exists underneath the outlined rock outcrop (20,000 Ωm) with an underlying conductor (~50 Ωm). Anomalous surface conductors exist within the profile and are labelled as 'Zone A' and 'Zone B; there is no obvious topographic features for either and both exhibit resistivity values of 5-50 Ωm. The deep resistor shown as the red zone (5,000-10,000 Ωm) represents the basement of the profile.

Figure 6b represents the ERI results for profiles ER3 and ER4. ER3 incorporates a flat terrain with no obvious associated topographic features and displays a maximum resistivity of 150 Ωm. Within the profile two anomalous zones exist as ‘Zone C’ and ‘Zone D’; these exhibit lower resistivity values relative (0-20 Ωm) to the deeper parts of the profile (50-150 Ωm). ER4 focuses on the right-hand side of the profile which depicts an anomalous conductive zone as ‘Zone E’ (0-10 Ωm). Other notable features is an anomaly marked by a pink dashed line and a profile basement as large red-orange features (5,000-10,000 Ωm).

Results for FEM data are displayed as Figure 7 as profiles F1, F2 and F3 all of which incorporate both the HC and PC data. F1 and F2 depict peaks in conductivity over the channel of ‘Gully 1’, indicated as the blue box. F3 depicts relatively higher values in the Horizontal coil (HC) and anomalous high-low values in the PC in the western part of the profile, this is illustrated as ‘Conductive Zone 1’

4.1.2 Site B

Site B incorporates four ERI surveys (ER5-8) and three FEM surveys (F4-6) over a gully in the South-East of the site, locations of the gully and geophysical surveys are depicted through Figure 8. It incorporates a moderately dipping slope to the South with minimal grass coverage in the east and moderate grass coverage to the west of the gully.

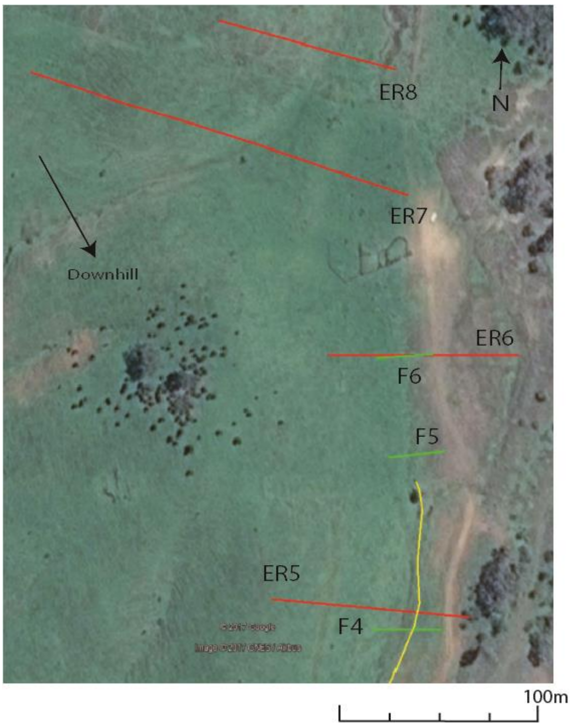

Figure 8. Google Earth image depicting the locations of ERI (Red lines) and FEM (Green Lines) surveys across an existing gully (Yellow line) for Site B. Surveys ER5 and F4 were conducted over the gully while F5 was 10m uphill, ER6 and F6 were 60m uphill, ER7 was 140m uphill and ER8 is 200m uphill from the head-cut

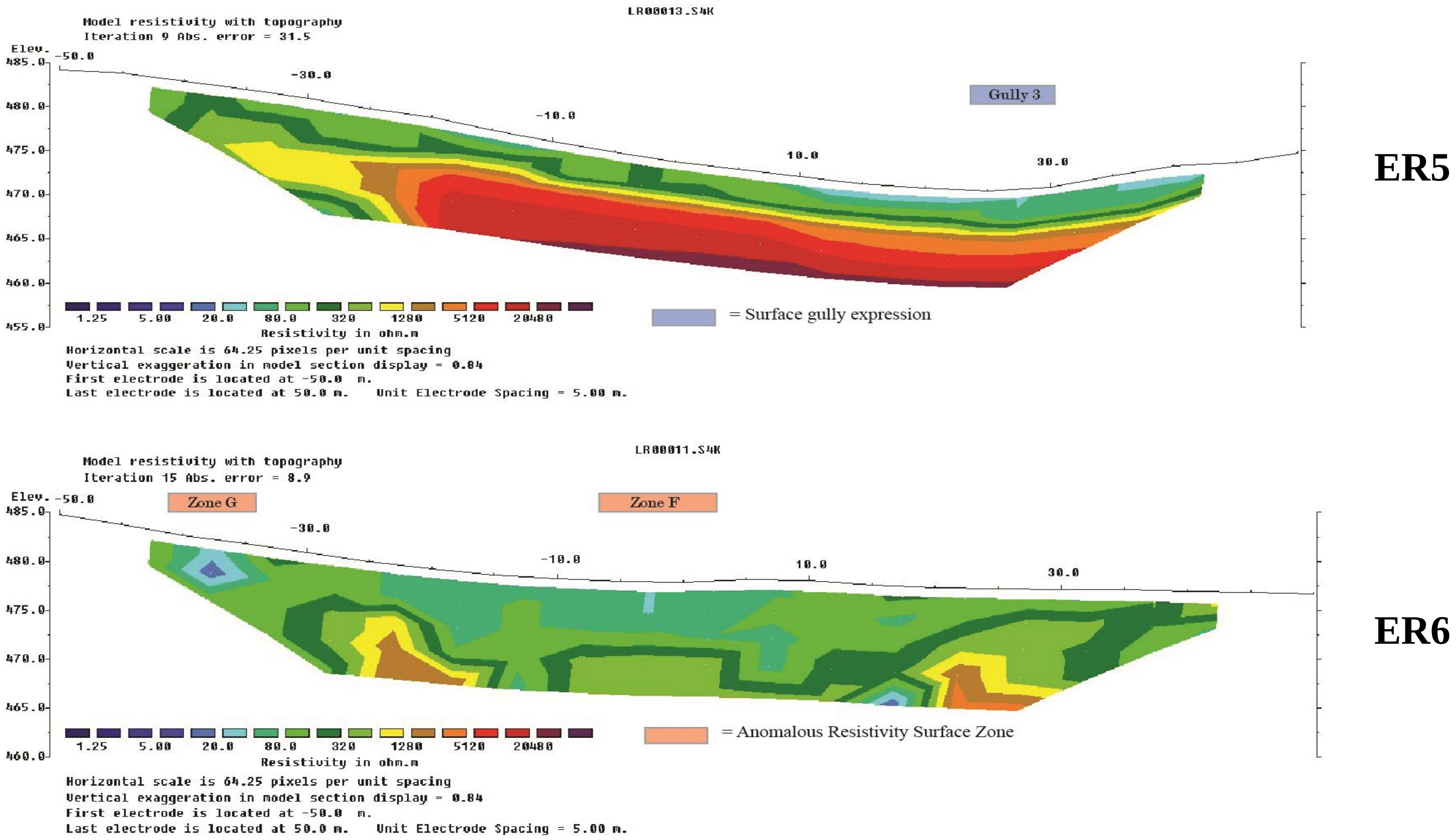

Figure 9a. Electrical Resistivity Imaging results for ER5 (Top) and ER6 (Bottom) for primary site B. Both profiles are 100m in length and incorporate the local topographic changes given via Trimble GPS system (2cm accuracy).

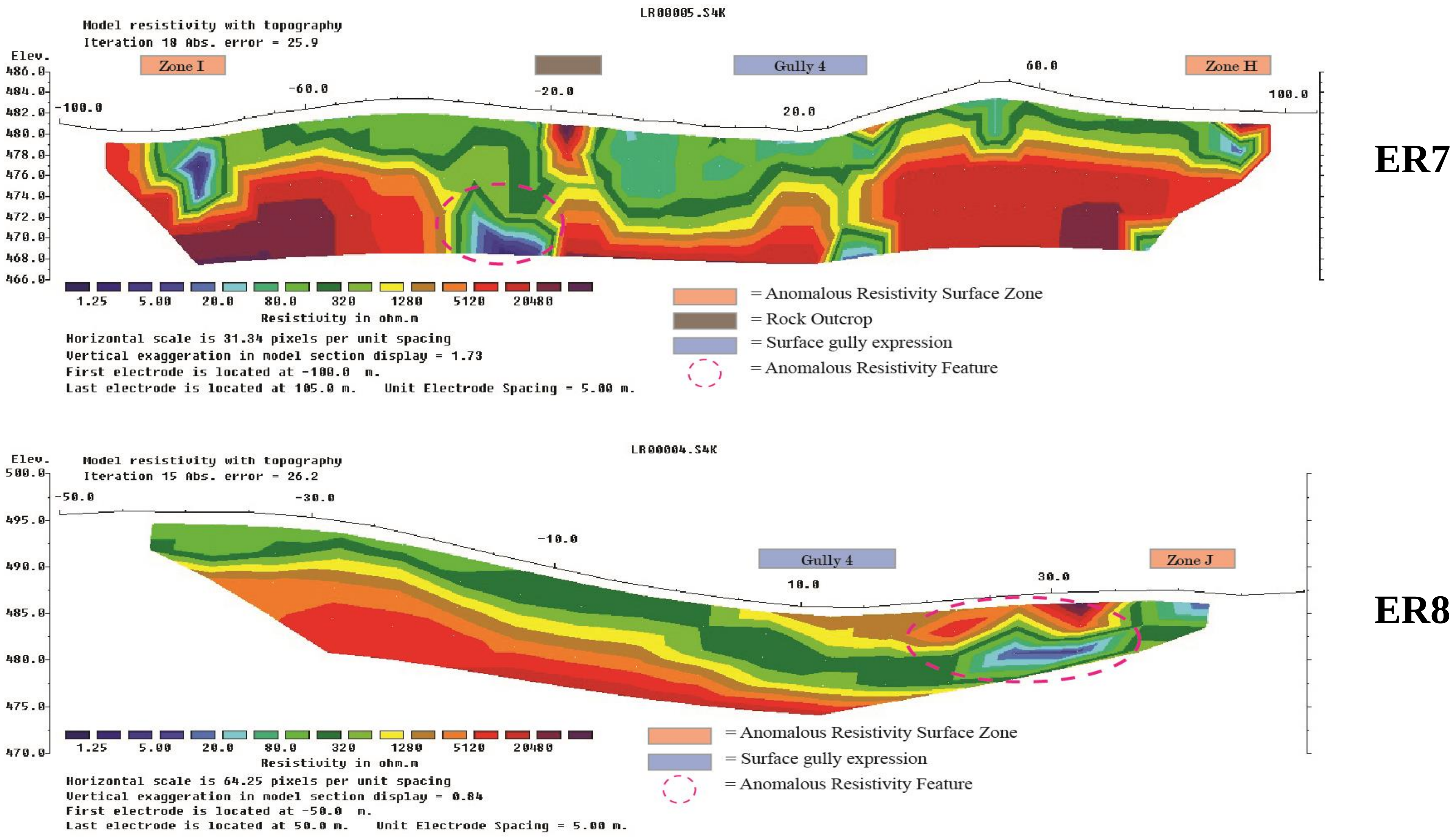

Figure 9b. Electrical Resistivity Imaging results for ER7 (Top) and ER8 (Bottom) for primary site B. ER7 is 200m in length and ER8 is 100m in length; profiles incorporate the local topographic changes given via Trimble GPS system (2cm accuracy).

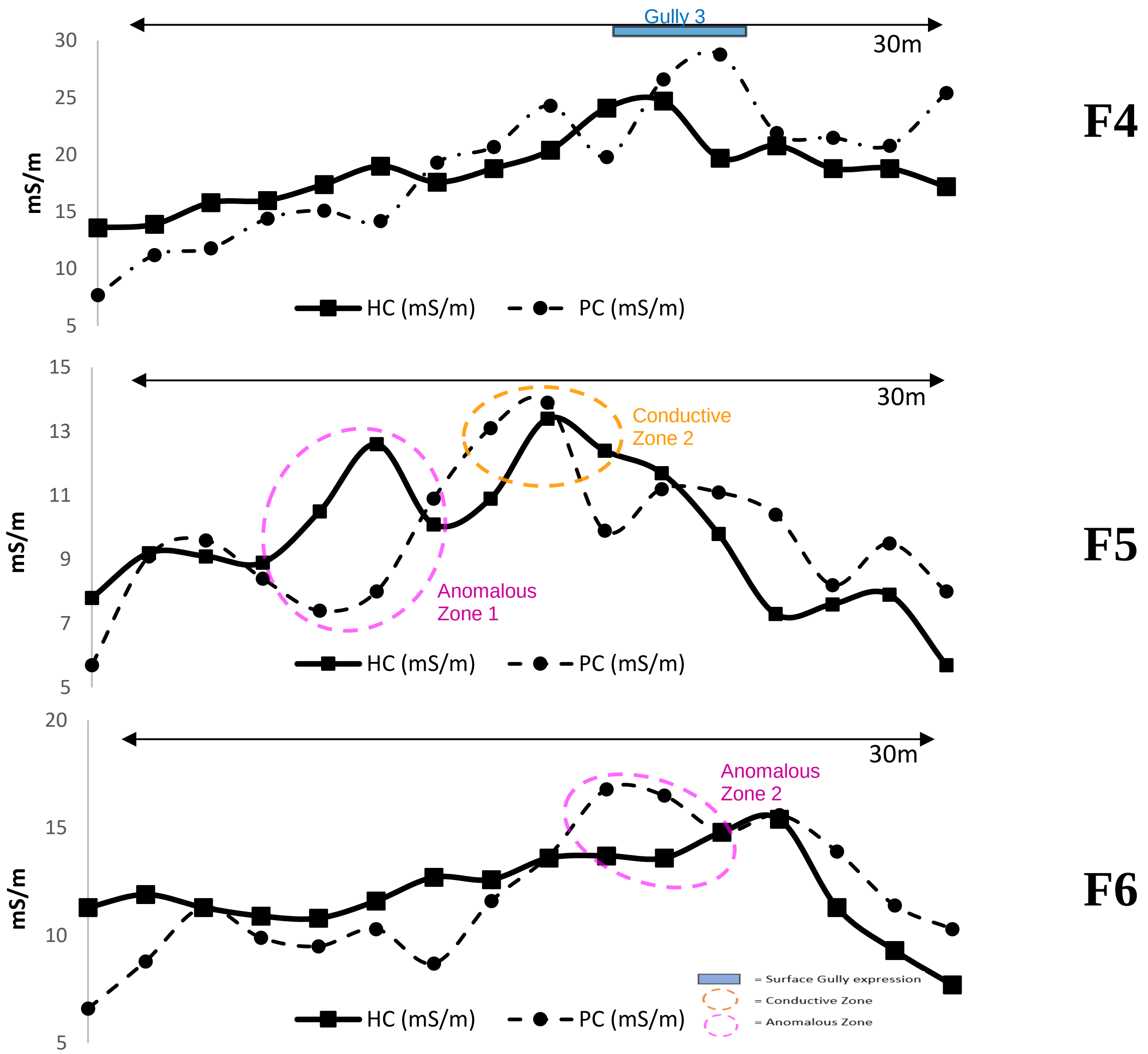

Figure 10. FEM results for profiles F4, F5 & F6 within site B. Vertical axis is in mS/m and the horizontal axis is in metres, distance between each data point is 2m. Obvious surface features that were encountered along survey lines are also illustrated.

Figure 9a represents the ERI results for profiles ER5 and ER6. ER5 crosses the gully depicted in Figure 8, within the profile a shallow conductive zone of ~5-20 Ωm exists and represents the intersected gully labelled as 'Gully 3'. The profile also depicts the shale basement as the deeper resistor of 20,000 Ωm. ER6 depicts two shallow conductive features labelled as 'Zone F' and 'Zone G' which exhibit resistivity values of 5-20 Ωm and 1-20 Ωm respectively. Both features aren't associated with any obvious topographic features indicative of fluid movement; Zone G is however on the slope of a hill which faces the east. The basement is depicted as the two deep yellow resistors (5,000 Ωm) within the profile, the separation of these incorporates much lower resistivity values of 300-500 Ωm.

Figure 9b represents the ERI results for profiles ER7 and ER8. ER7 depicts two surface conductors on either side of the profile labelled 'Zone H' and 'Zone I'; both exhibit resistivity values of ~1-10 Ωm. Within the profile a rock outcrop of the shale basement was also encountered and is representative of the surface resistor marked as “Rock Outcrop”. The profile also illustrates a deeper conductive anomaly, marked as a dashed pink circle that separates the basement resistor. ER8 involves a single surface conductor anomaly labelled as ‘Zone J’ (5-20 Ωm) on the edge of the measured profile. An anomaly also exists and is outlined by a pink dashed circle. ‘Gully 4’ represents a field observation along the profiles, it was not measured for potential head-cut retreat/LPP.

Results for FEM data are displayed as Figure 10 as profiles F4, F5 and F6 all of which incorporate both the HC and PC data. F4 depicts peaks in the HC and PC values at the same location that the survey crosses ‘Gully 3’ which is shown as a shaded blue box. F5 illustrates ‘Anomalous Zone 1’ which depicts a peak in the HC and a trough in the PC. The profile also incorporates ‘Conductive Zone 2’ in the centre of the profile which exhibits peaks in the HC and PC values. F6 incorporates an anomalous peak in the PC values relative to the background levels; this is illustrated as a pink dashed circle labelled ‘Anomalous Zone 2’.

4.1.3 Site C

Site C incorporates four ERI surveys (ER9-12) and four FEM surveys (F7-10) over a gully in the Centre-North of the site, locations of the gullies and geophysical surveys are depicted through Figure 11. It incorporates a moderate-steep dipping slope to the South-West with high density grass, sporadic tree and occasional bare ground coverage.

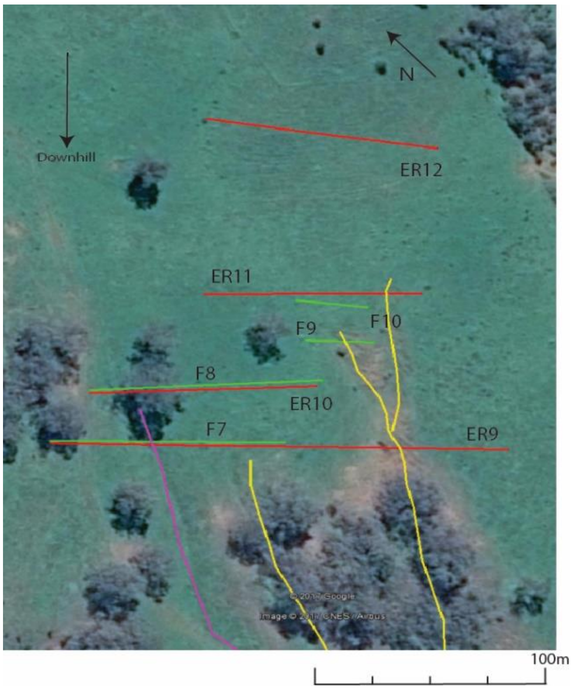

Figure 11. Google Earth image depicting the locations of ERI (Red lines) and FEM (Green Lines) surveys across existing gullies (Yellow lines) for Site C . Surveys ER9, ER11 and F9 were conducted over an existing gully while ER10 and F8 were 30m uphill, ER11 and F10 were 80m/20m, ER12 was 160m/90m uphill from all gully head-cut respectively. The purple line represents another surface expression of a gully which was detected on the edge of uphill surveys, it is not considered a targeted feature.

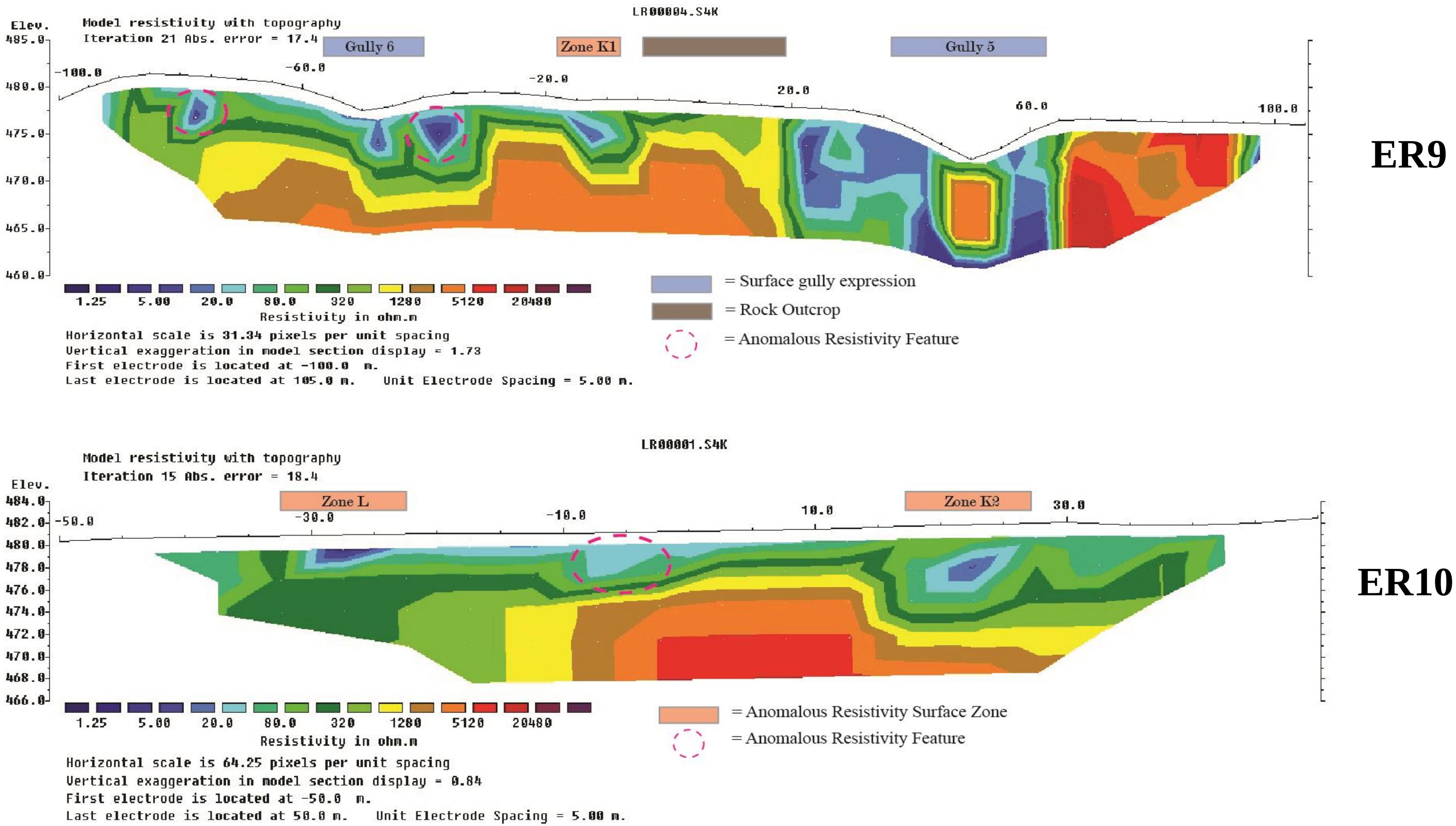

Figure 12a. Electrical Resistivity Imaging results for ER9 (Top) and ER10 (Bottom) for primary site C . ER9 is 200m in length and ER10 is 100m in length; profiles incorporate the local topographic changes given via Trimble GPS system (2cm accuracy).

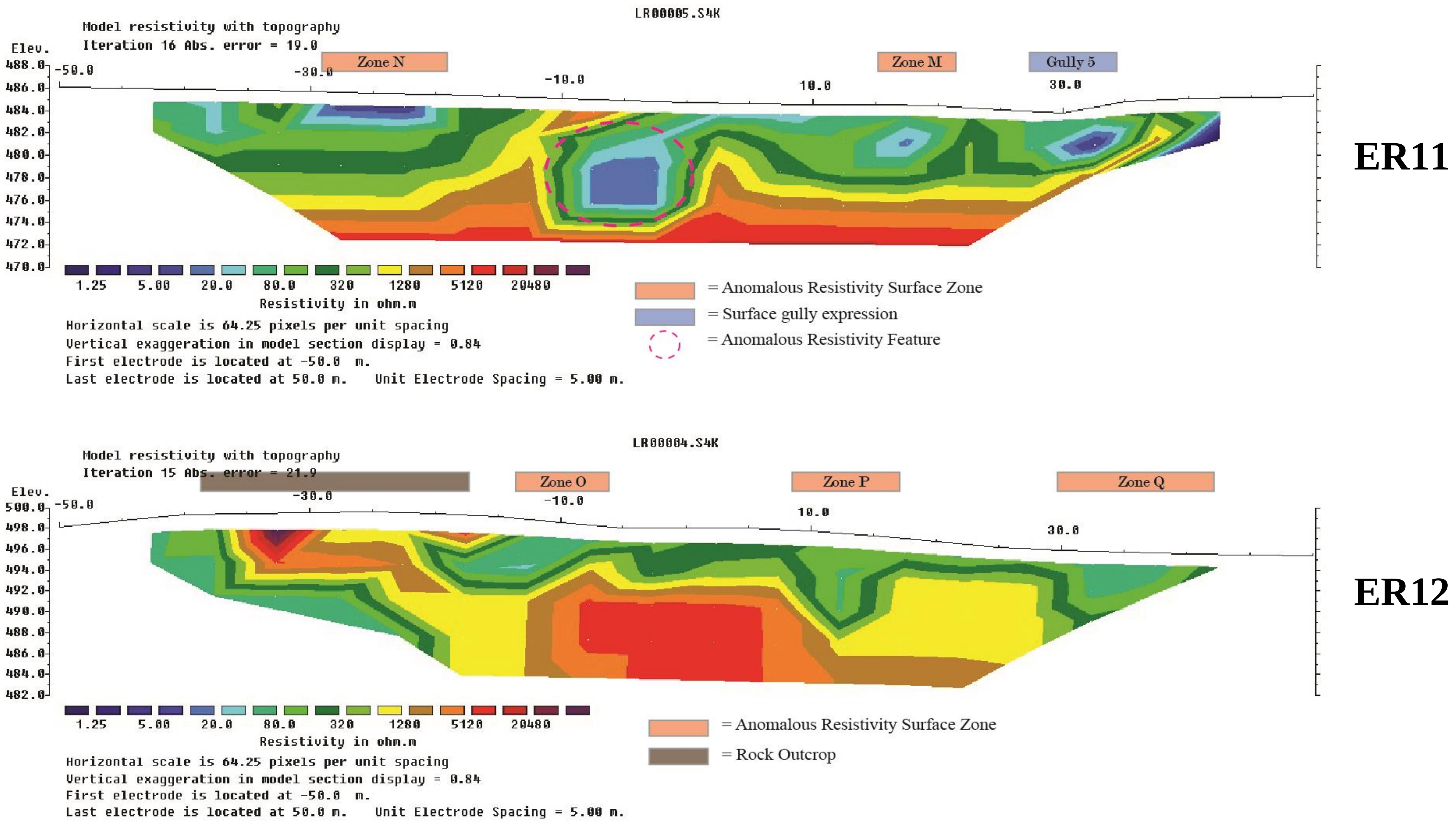

Figure 12b. Electrical Resistivity Imaging results for ER11 (Top) and ER12 (Bottom) for primary site C. Both profiles are 100m in length and incorporate the local topographic changes given via Trimble GPS system (2cm accuracy).

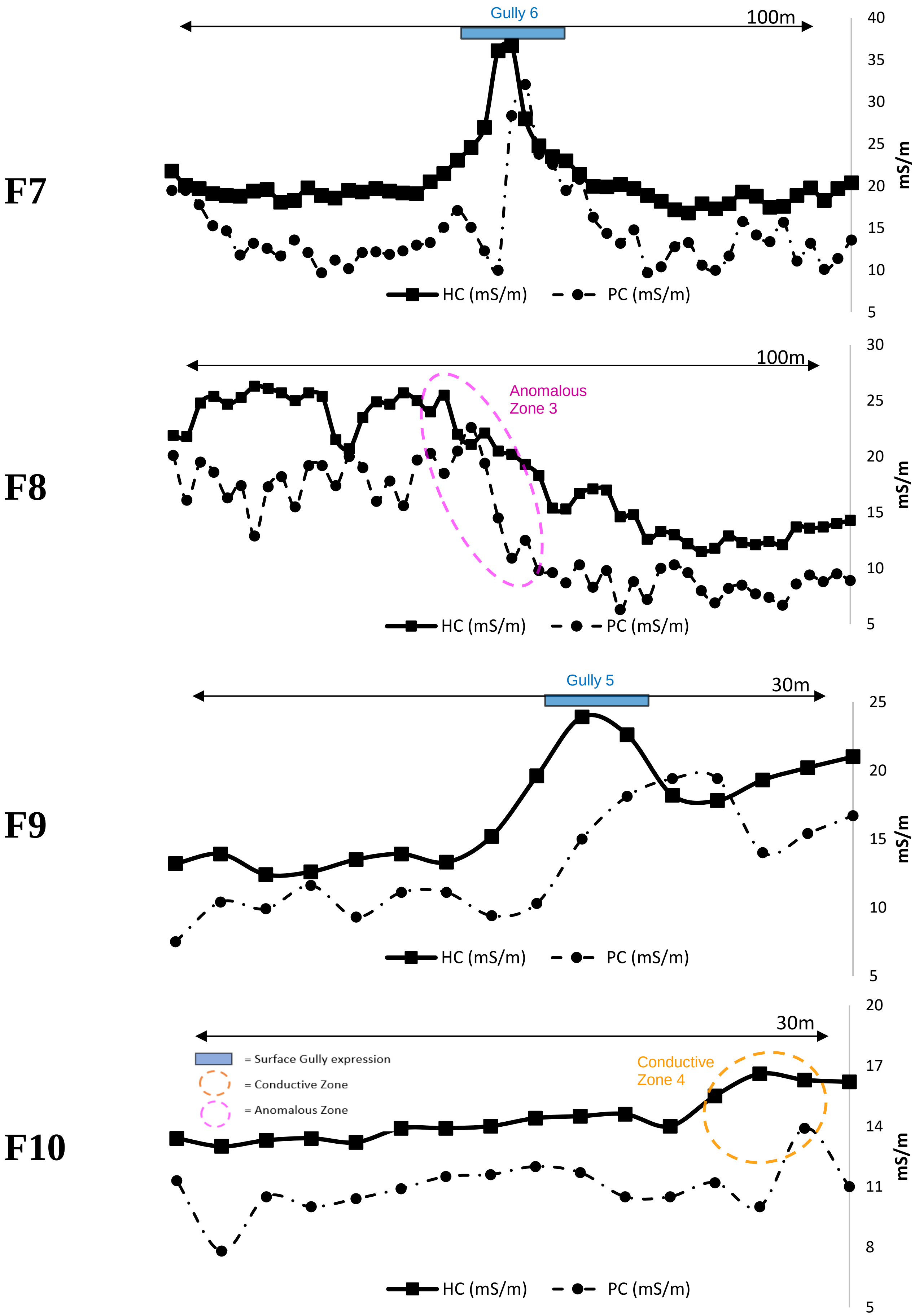

Figure 13. FEM results for profiles F7, F8, F9 & F10 within site C. Vertical axis is in mS/m and the horizontal axis is in metres, distance between each data point is 2m. Obvious surface features that were encountered along survey lines are also illustrated

Figure 12a represents the ERI results for profiles ER9 and ER10. ER9 intersects two gullies shown as ‘Gully 5’ and ‘Gully 6’ which also depicts the associated lows in topography seen on the profile; both gullies exhibit resistivity values of 1-20 Ωm. ‘Gully 5’ also depicts a large rectangular resistor in the middle of a conductor. Profile ER9 also illustrates a conductive zone with no associated topographic changes labelled as ‘Zone K1’ which represents a small surface conductor of 1-10 Ωm between the two gullies. Electrical response of the basement varies between 5,000 Ωm in the west of the profile to 20,000 Ωm in the east. Two conductive anomalous zones also exist which are outlined by dashed pink circles, both depict 1-10 Ωm. ER10 depicts two shallow conductive zones as ‘Zone K2’ and ‘Zone L’ both of which exhibit conductive values of 1-20 Ωm. An anomalous zone is indicated by the pink dashed circle and depicts a conductive feature of ~20 Ωm. The basement is also represented as the resistor at the bottom of the profile with an electrical response of 10,000 – 20,000 Ωm.

Figure 12b represents the ERI results for profiles ER11 and ER12. ER11 intersects ‘Gully 5’ in the east of the profile and depicts similar values to ER9 as 1-20 Ωm with a topographic low. The profile also depicts two surface conductors labelled as ‘Zone M’ with resistivity values of 5-20 Ωm and ‘Zone N’ with 1-10 Ωm. A large conductor that intrudes into the basement (20,000 Ωm) has been classified as an anomalous resistivity feature with values of 5-20 Ωm. ER12 depicts three surface conductors as ‘Zone O’, ‘Zone P’ and ‘Zone Q’ which are relatively more resistive than other outlined “anomalous Resistivity Surface Zones”. ‘Zone O’ exhibits resistivity values of 10-20 Ωm, ‘Zone P’ and ‘Zone Q’ are more resistive displaying values of 20-80 Ωm. Rock outcrops that were encountered are representative of the basement depicting resistivity values of 20, 000 Ωm.

Results for FEM data are displayed as Figure 13 as profiles F7, F8, F9 and F10 all of which incorporate both the HC and PC data. F7 shows a distinct peak in both HC and PC in the center of the profile which identifies the location of ‘Gully 6’. F8 shows a sharp change from high to low values in conductivity for both HC and PC at ‘Anomalous Zone 3’. F9 depicts a peak in the HC and PC conductivity values at the same location as ‘Gully 5’. F10 shows a small peak in the HC and a moderate peak in the PC in the eastern section of the profile, this is labelled as ‘Conductive Zone 4’.

4.2 Secondary Sites

4.2.1 Site D

Site D incorporates two ERI surveys (ER13 & 14) and one FEM survey (F11) over a gully in the North of the site, locations of the gully and geophysical surveys are depicted through Figure 14. It incorporates a moderately dipping slope to the South-West with high density grass and sporadic tree ground coverage.

Figure 14. Google Earth image depicting the locations of ERI (Red lines) and FEM (Green Lines) surveys across an existing gully (Yellow line) for Site D . Survey ER13 was conducted 25m uphill of the gully head-cut while ER14 and F11 were 55m uphill.

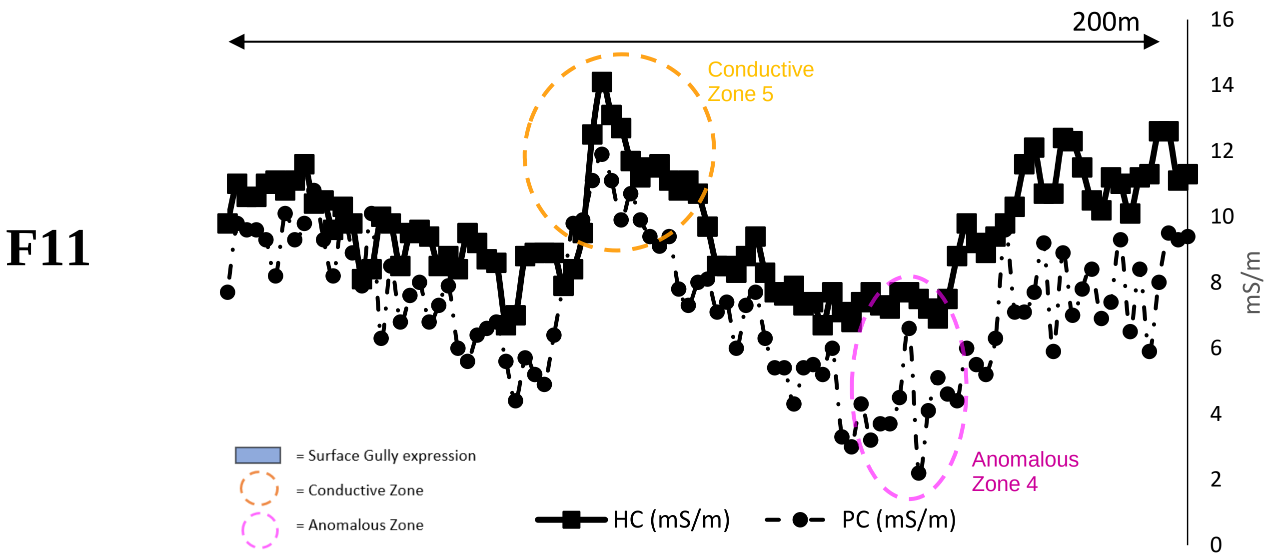

Figure 15. FEM results for profile F11 for site D. Vertical axis is in mS/m and the horizontal axis is in metres, distance between each data point is 2m. Obvious surface features that were encountered along survey lines are also illustrated.

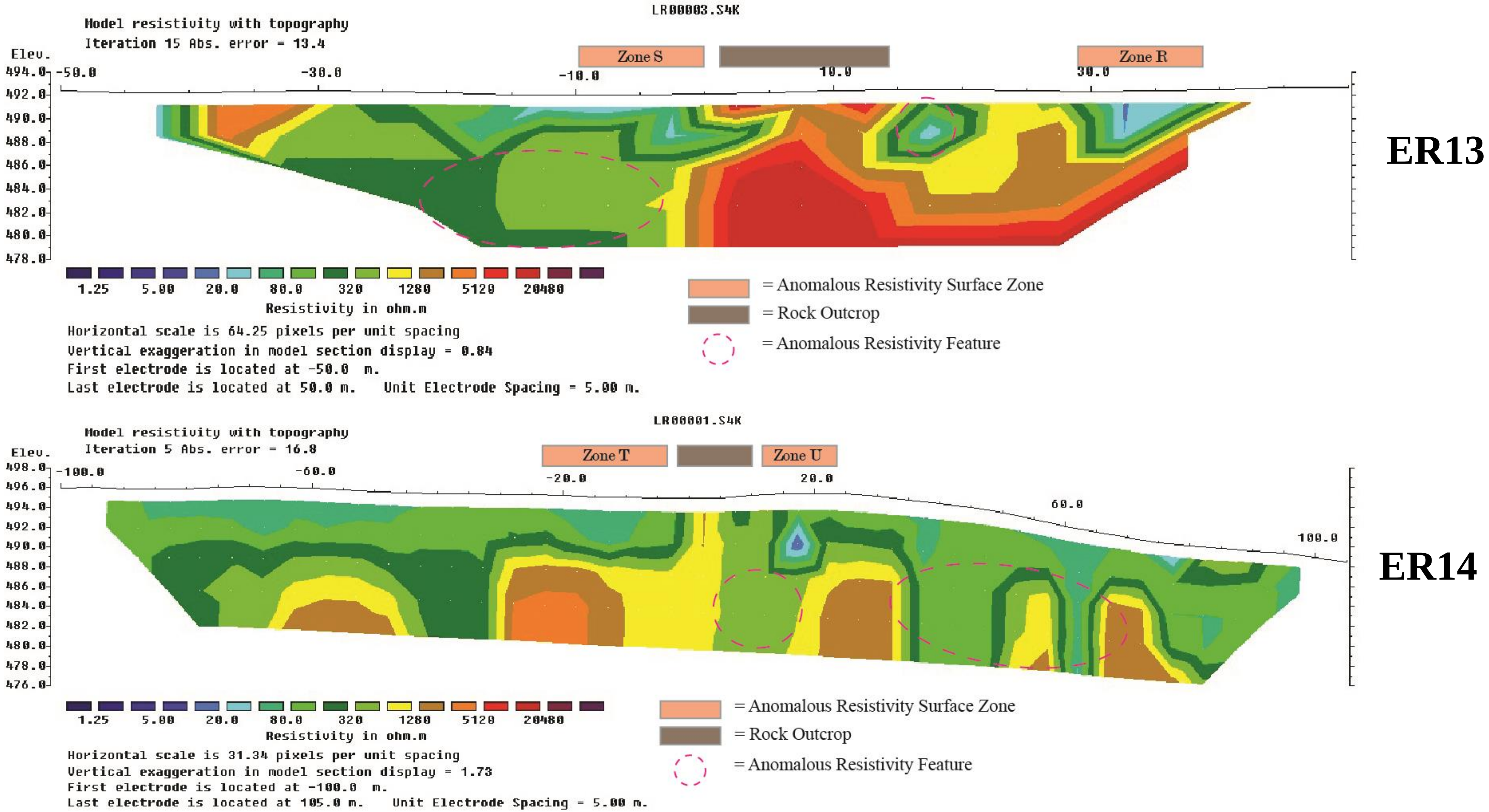

Figure 16. Electrical Resistivity Imaging results for ER13 (Top) and ER14 (Bottom) for secondary site D. ER13 is 100m in length and ER14 is 200m in length; profiles incorporate the local topographic changes given via Trimble GPS system (2cm accuracy).

Results for FEM data are displayed as Figure 15 as profile F11 all of which incorporate both the HC and PC data. F11 illustrates a peak in conductivity within 'Conductive Zone 5' relative to the background levels of. 'Anomalous Zone 4' depicts a divergence between the PC and HC, a high then low value occurs within the PC line while no obvious change occurs within the HC line.

Figure 16 represents the ERI results for profiles ER13 and ER14. ER13 depicts two shallow conductors as 'Zone S' and 'Zone R' and another anomalous conductor which is circled; all of which exhibit electrical responses of 5-20 Ωm. The western section of the profile illustrates an anomalous area (300-500 Ωm) shown as a dashed red circle, the basement rock (10,000-20,000 Ωm) is absent. ER14 similarly depicts two shallow conductive zones shown as 'Zone T' and Zone U' with an outcrop of basement shale (5,000 Ωm) between them. 'Zone T' is shown with relatively more conductive values of 50 Ωm while 'Zone U' depicts a strong conductor of 5-10 Ωm. This profile also illustrates numerous zones in which the basement appears to be segmented by low resistive zones of 300-500 Ωm, examples of these are represented by the red dashed circle

4.2.2 Site E

Site E incorporates two ERI surveys (ER15 & 7) over a gully that stems off a major gully system in the East of the site, locations of the gully and geophysical surveys are depicted through Figure 17. It incorporates a moderately dipping slope to the South with minimal grass ground coverage.

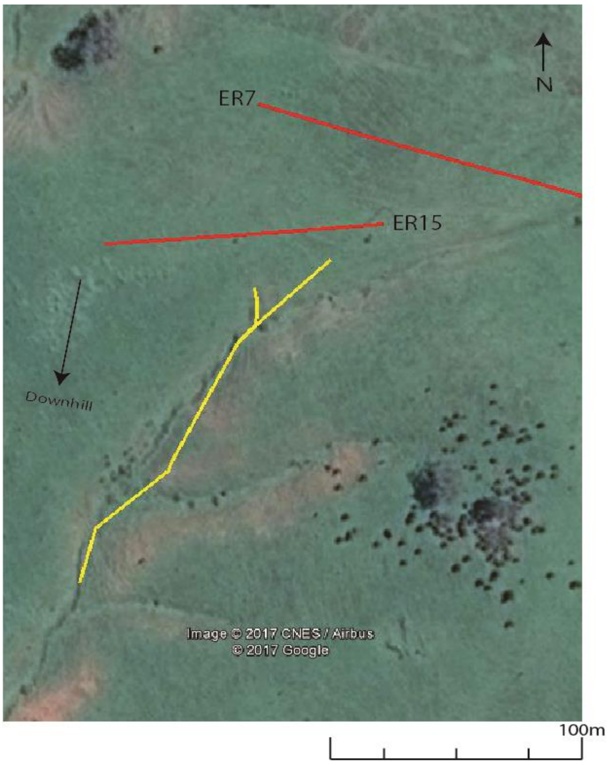

Figure 17. Google Earth image depicting the locations of ERI (Red lines) surveys across an existing gully (Yellow line) for Site E. Survey ER15 is 20m uphill from the head-cut while ER7 is 60m uphill

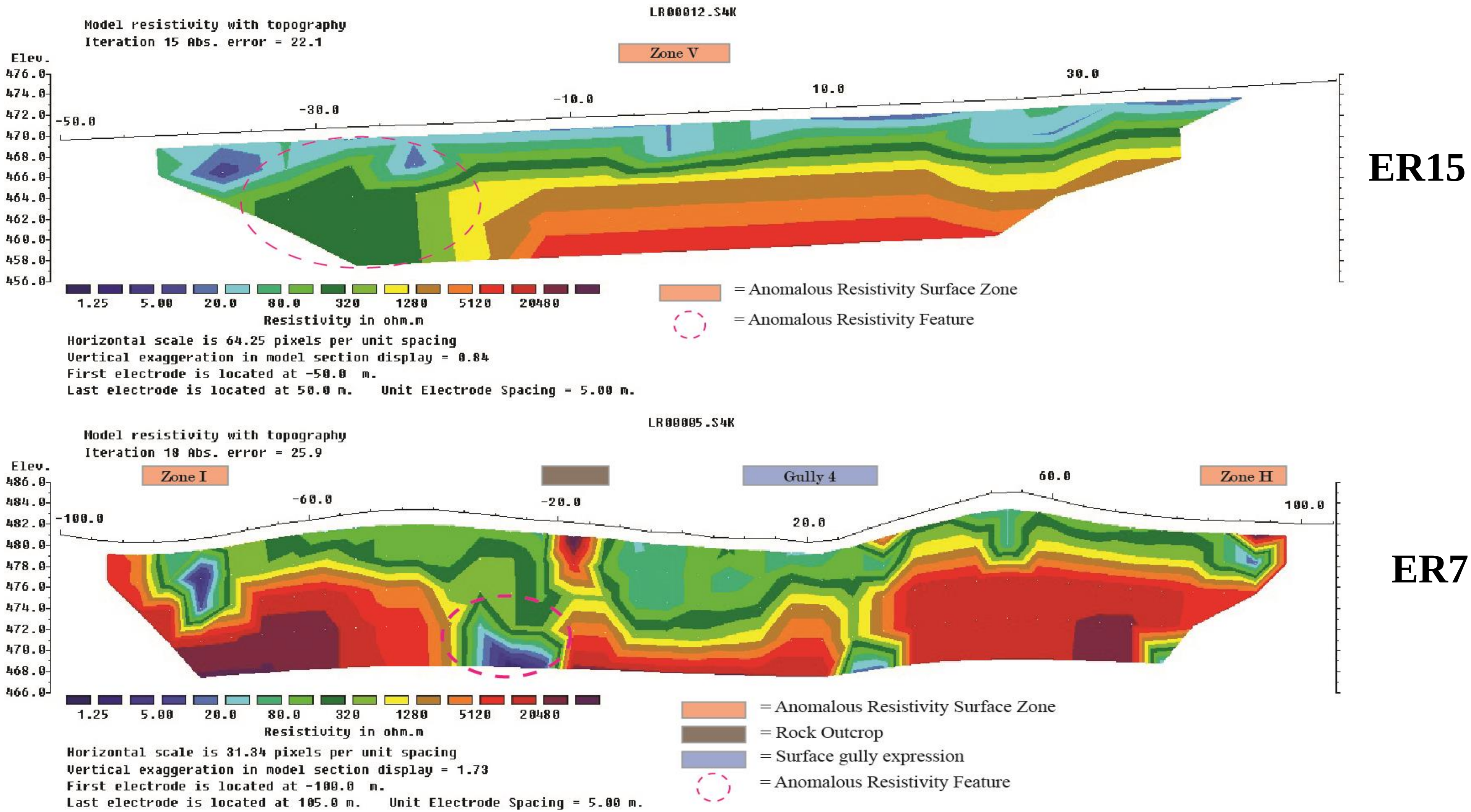

Figure 18. Electrical Resistivity Imaging results for ER13 (Top) and ER14 (Bottom) for secondary site D. ER13 is 100m in length and ER14 is 200m in length; profiles incorporate the local topographic changes given via Trimble GPS system (2cm accuracy).

Figure 18 represents the ERI results for profiles ER15 and ER7. ER15 depicts a conductive surface anomaly with no associated topographic changes labelled as 'Zone V'; its electrical response is 5-20 Ωm. An anomalous resistivity zone exits in the western part of the profile which depicts low-moderate resistivity values of 300-500 Ωm shown as the green coloured feature within the pink dashed circle. This is relatively lower than the associated basement (5,000-10,000 Ωm) seen as the resistive red feature at the bottom of the central and eastern parts of the profile. Profile ER7 has been referred to before in site B, this particular site focuses on 'Zone I' which represents a shallow conductive feature with an electrical response of 1-10 Ωm. Topography associate with 'Zone I' appears to be a shallow dip, this topographical feature was also observed in the field.

4.3 Background Survey

To compare the measure anomalous shallow conductors to the average resistivity of background soils with no topographical features or associated gullies, an ERI survey was conducted within the area study area to the South-East of site C depicted as a bright orange line in Figure 4. The results of which are depicted as Figure 19.

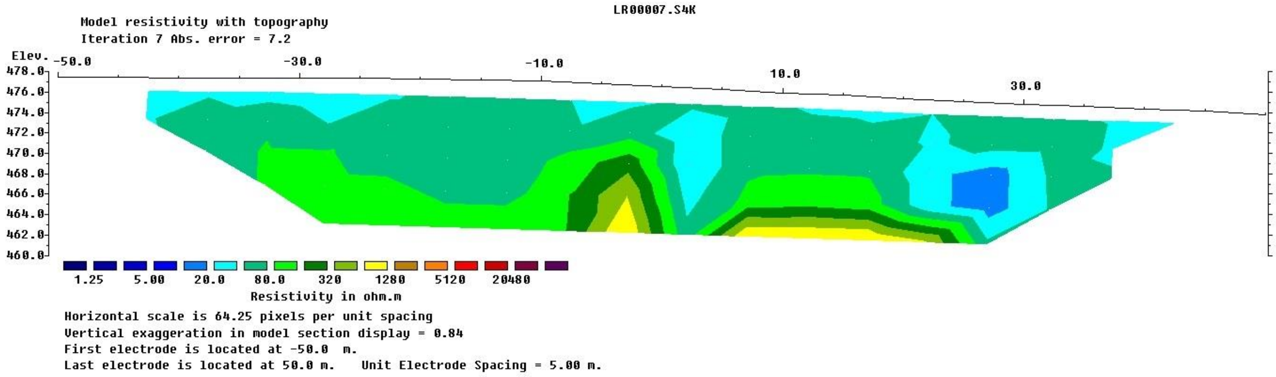

Figure 19. ERI survey which depicts the background resistivity values for the study site. Profile was conducted over an area with devoid of gullies below or above the location; refer to 'Bright Pink Line' on Figure 4 for exact location within the study site.

The background resistivity of shale soils is shown through Figure 19 as the light blue to light green areas; these depict resistivity values of 60-300 Ωm and extend across the whole profile as a 5-15m soil layer. A single conductor is depicted at a depth of ~10m within the subsurface related to a nearby gully ~20m east, other features include yellow resistors at the base of the profile are representative of the shale basement layer.

Chapter 5: Discussion

As stated previously within this investigation there is a growing necessity for predictive tools of significant environmental and production issues; not just including gullying of soils but for weather patterns, climatic conditions, crop yields and risk assessments (Stein and LaTray, 2002). Predictive models exist for a large majority of factors associated with agricultural production and urban planning, although due to the complexities with head cut migration the ability to predict the pathway of gullying is extremely limited (Poesen et al., 2003). This investigation of head-cut migration aims to produce an applicable field method to predict future pathways using electrical geophysical to trace LPP. The results given as the ERI and FEM profiles exhibit near-surface shallow conductive anomalous zones uphill from gully head-cuts with no obvious associated topographic variations.

To link and construct these zones as LPP; integrated figures for each study site were generated with interpretations drawn over them; these are shown as figures 20-24. Evaluation of the proposed method will incorporate direct comparisons with currently existing gully assessment techniques regarding quality and efficiency in data collection. It should be noted that due to the time allocated for the study it is impossible to completely assess the technique as significant GHR can take between months to years; this is dependent on climatic and topographic conditions (Samani et al., 2016). Comparison will be based on the ability and benefits of other techniques and the proposed benefits of the geophysical location of LPP.

5.1 Data Interpretations

To visualise longitudinal preferential pathways ERI profiles for each site have been compiled and integrated to depict the connection between anomalous conductive features. Integrated ERI results incorporates interpreted LPP’s shown as dashed black lines of varying thicknesses ending with open squares. Open squares are indicative of the limits of interpretation, above this point there is no data to continue the LPP further uphill. Varying thicknesses of the dashed lines are indicative of the confidence of the interpretation, the thicker the line the higher the confidence. FEM results aren’t displayed on the integrated figures below but are still associated with the interpreted pathways and will also be discussed. Within the ERI results an ‘Over-Under’ feature was identified in several profiles, this is interpreted to be a weathering pattern associated to the area, near rock units are weathered through hydrological processes.

5.1.1 Targeted Conductors

To determine significant resistivity values which represent points along an LPP the profile in Figure 19 was conducted to measure background soil resistivity values. The average soil resistivity for the study site is 60-300 Ωm and values >1000 Ωm are associated with the shale basement. It was hypothesized that targeted conductor's representative of LPP would exhibit values of 1-40 Ωm; based on the results of Figure 19 this range is appropriate for determining the significance of anomalous features. Conductors within this range are considered significant and were labelled as 'Zones' to easily represent linkages between anomalous conductors in the subsurface. Integrated profiles which have a high confidence in the interpreted LPP are depicted bold dashed lines and labelled as "LPP#" while lower confidence models are thinner and are not labelled. Although in cases were interpretations have been made through more resistive zones FEM data has supported the LPP traced line as well as relative differences within the same profile.

5.1.2 Site A Interpretation

Figure 20 depicts the results of the integration of the ERI surveys conducted in Site A, interpreted LPP traces are depicted as the black dashed lines illustrated through the profiles and locational image. Significant Conductive zones (A-E) are outlined in Figure 6a and 6b of the results section; these match the targetable parameters representative of zones of higher saturation expected for an LPP.

The primary focus for this site was a moderate gully referred to as 'Gully 1' which is depicted as the yellow line and is associated to the bold dashed trace labelled as LPP1 connecting the head cut of the gully to a series of uphill anomalous conductive zones. LPP1 was traced through shallow conductors that matched the targeted electrical response outlined in the section above, the trace for LPP1 are as follows; **'Gully 1' → Zone A → Zone C → Zone E**. Majority of profiles depict singular conductive zones which are interpreted as points along an LPP, although in ER3 there are several conductors. The Northern most conductor is related to the large dam feature seen in the locational image to the North of ER3, while the smaller conductor to the south of Zone C involved less conductive values. Zone E is interpreted as the edge of detection and the conductor is considered a singular anomalous zone. Interpretation of LPP1 is given high confidence based on similarities between the predicted pathway and existing landforms erosional pathway styles, topographical conformity and correlation to targeted conductive zones.

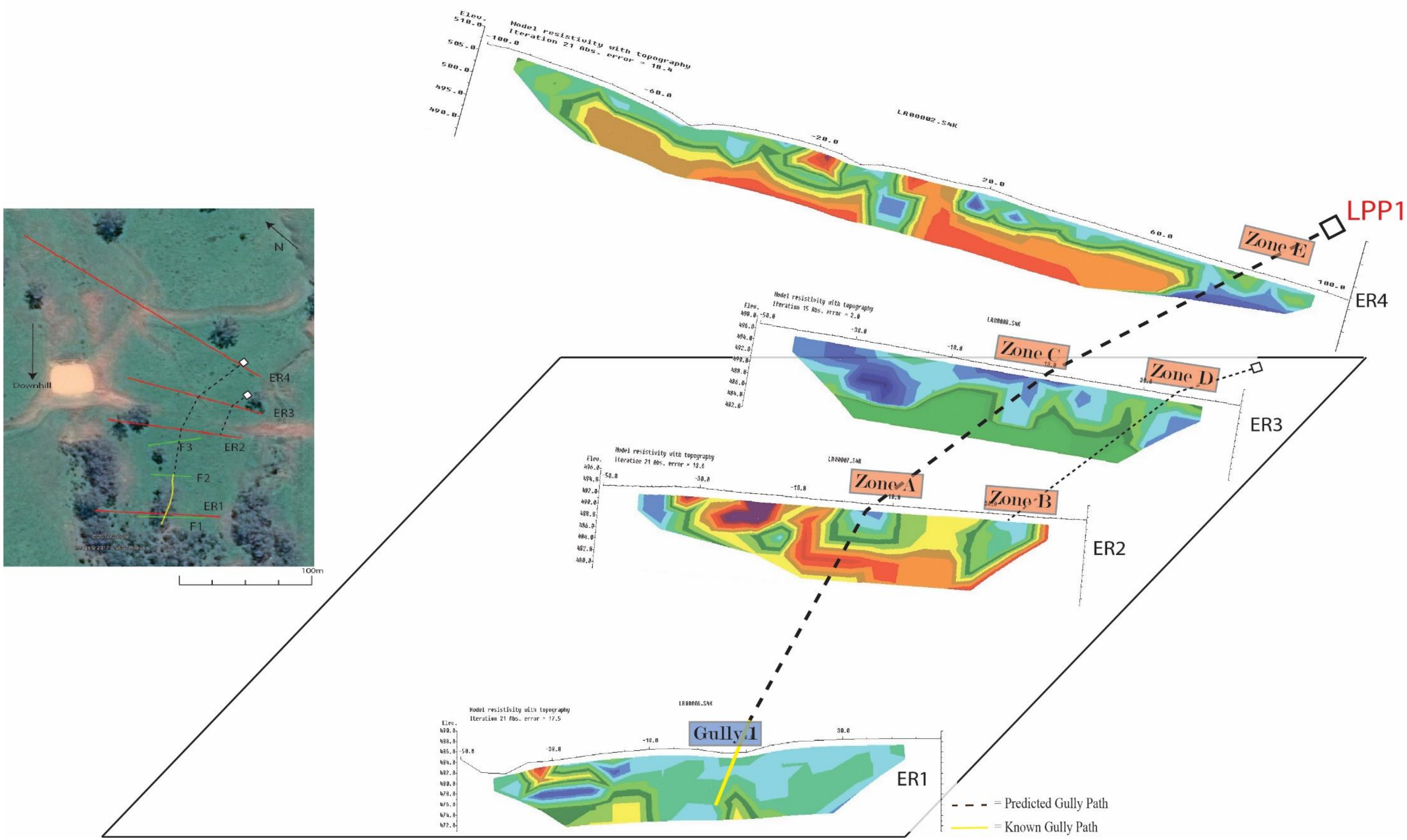

Figure 20. Integrated ERI results with an associated Google Earth image for site A; positions and orientations of each profile are relative to on ground positions shown as the small image to the top left of the figure.

Another thinner trace which is associated with a lower confidence is also shown in Figure 20 which connects zones B and D as an interpreted LPP. Based on the topography and form of LPP1 it is interpreted that these features are potentially linked with Zone E but minimal confidence was given to this interpretation; it has been interpreted as a potential fork or eventual discontinuous gully.

FEM data for site A is shown in the results as Figure 7; profiles F1 and F2 support the positioning of 'Gully 1' in Figure 20 through outlined obvious conductive peaks in both the HC and PC. Further uphill F3 depicts an anomalous conductive zone in the PC in the general area which LPP1 intersects with Zone A, this supports the link between Head cut and Zone A but the exact positioning couldn't be derived purely from FEM.

5.1.3 Site C Interpretation

Site C is considered the most complicated area within the investigation due to the presence of multiple gullies represented as solid yellow lines which are then associated to multiple LPP traces shown as dashed black lines; all this is depicted in the integration of ERI data for site C as Figure 21. Interpretations for LPP traces vary between the two gullies, the primary focus for site C was the identified central gully while the secondary focus was 'Gully 5' seen as the easterly landform.

The primary gully outlined in the center of site C was located using GPS/field observations and then included into the dataset as the solid yellow line. In terms of the associated interpretations the gully is linked with numerous uphill anomalous conductors which is represented through a bold dashed line is traced through and labelled as LPP2. The trace for LPP2 is as follows: **Gully 5 → Zone K1 → Zone K2 → Zone N → *Inconclusive***. Associated zones K1, K2 and N all fall within the targetable range for conductive anomalies representative of points along a LPP. Zone K1 is considered significant due to its relatively high conductivity and proximity to the gully head cut. Links to Zone K2 and N as a continuation of LPP2 are based on the high conductivity values and the conformity of the LPP to the terrain/slope. Past Zone N to ER12 the confidence in the predictive model is minimal due to lack of data; numerous interpretations can be made and so it is suggested that for solid interpretations of LPP2 further ERI surveys are necessary. Links associated between conductive zones K-N as LPP2 are interpreted with high confidence, as is suggested by the bolded trace. It conforms to the topography of the site as a slope to the South-West and reflects similar aspects to well-developed gullies within proximity.

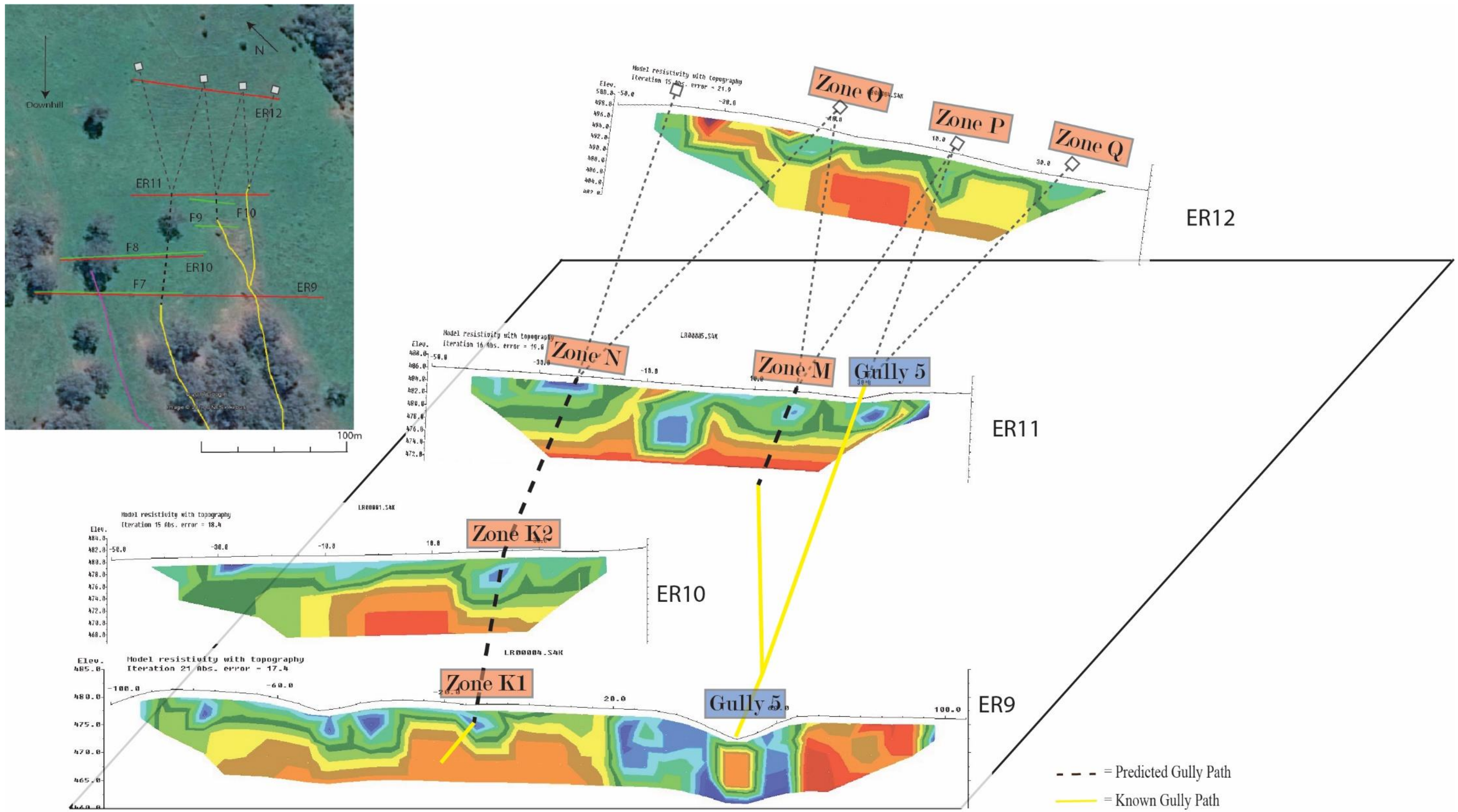

Figure 21. Integrated ERI results with an associated Google Earth image for site C; depicting the interpreted LPP shown as the black dashed line which intersects each profile through a shallow conductor.

‘Gully 5’ incorporates two distinct forks represented in Figure 21 as a western and eastern fork. For the western fork the head cut occurs downhill of the eastern fork and is associated with a confident interpretation of an LPP. This link is interpreted between the identified head cut and Zone M; this is based on the anomalous conductor occurring within the targetable range and the conformity to the south-westerly downhill curvature of the site. Past this point interpretations are inconclusive due to multiple potential pathways represented as the two thin dashed lines branching from Zone M. The channel of the Eastern fork of the secondary gully is detected through ER11 and is shown on Figure 21. Links between the head cut of this channel to uphill locations cannot be confidently traced due to the lack of data mentioned earlier, this has resulted in numerous potential pathways being interpreted.

FEM data for site C is shown as Figure 13 in the results section as profiles F7-F10. It was found in this data set that only obvious topographic landforms that would normally be associated with changes in conductivity could be confidently identified. This is outlined as profiles F7 and F9 which depict conductive peaks that occur within the gully channel; as for F8 and F10 which were uphill of gullies distinctive peaks could not be delineated from the background conductivity. Anomalous zones outlined could not be confidently interpreted as representative of an LPP conductor.

‘Gully 6’ is depicted as the pink line the locational image, no investigation was carried out on this gully although it is interpreted to be associated with site D. Although it does provide further evidence for associated shallow conductors above head cuts.

5.1.4 Site E Interpretation

Figure 22 depicts the integration of the two ERI surveys conducted for site E; a confident LPP trace is interpreted and shown as the dashed black line which initiates at the gully shown as the yellow line below ER15. The traced LPP is as follows: **Gully → Zone V → Zone I**. The location of the head cut is inferred as the end of the yellow line in Figure 22; this was determined and outlined through GPS locational data. It is interpreted to be linked as a LPP with a shallow conductor ~10m uphill referred to as Zone V; this is based on a targetable conductive anomaly detected within the ERI which conforms to the large scale slope and topography of the site compared to other detected shallow conductors. Other similar conductors on ER15 are too distant from the head cut to be reasonable linked too. Zone V is then interpreted to be associated as an LPP with Zone I a larger conductive feature; this interpretation is partially based on field observations in which a wide depression is experienced sloping to the South-West. Relative differences between the conductive anomalies can be explained by surveys being conducted in different seasons.

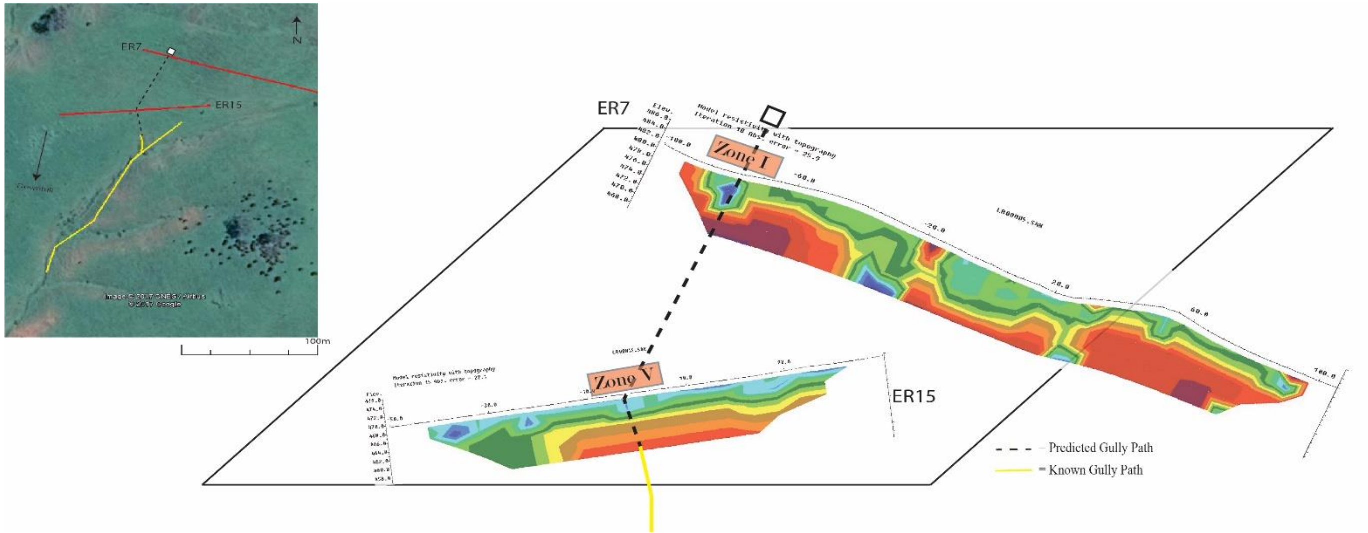

Figure 22. Integrated ERI results with an associated Google Earth image for site E; depicting the interpreted LPP shown as the black dashed line which intersects each profile through a shallow conductor

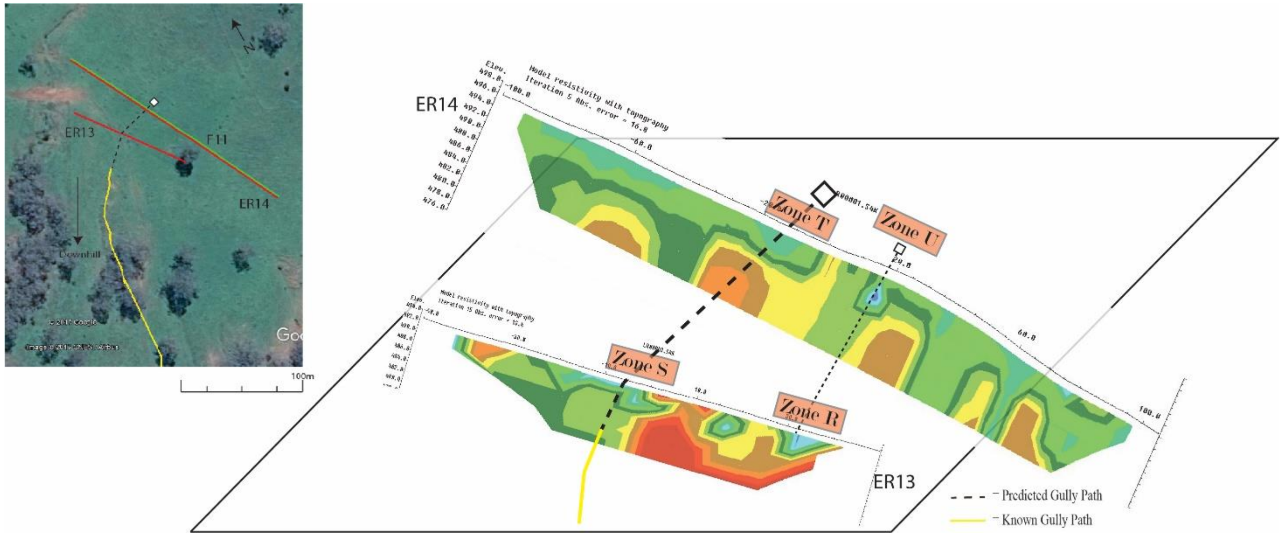

Figure 23. Integrated ERI results with an associated Google Earth image for site D; depicting the interpreted LPP shown as the black dashed line which intersects each profile through a shallow conductor.

5.1.5 Site D Interpretation

Interpretations of the results for Site D are shown as Figure 23 which depicts both ERI surveys with interpreted LPP's traced through identified conductive zones. The focus for this site is a singular gully represented as a solid yellow line seen in both the interpretation and locational image of Figure 23; the moderately confident traced LPP is interpreted as follows: **Gully → Zone S → Zone T**. The association as an LPP between the gully and conductive anomaly Zone S is based on the targetable conductivity values and the proximity of ER13 to the gully. Further interpretation is continuation of the LPP through Zone T which is ~40m uphill. Reasoning behind this pathway is relation to the downhill slope/topography as well as the relatively more conductive values of the shallow conductor to the rest of the profile. Although the conductive values of Zone T are more resistive than previous identified conductors and represent the edge of the targetable conductors FEM data shown as F11 on Figure 16 depict a conductive peak in the HC and PC as 'Conductive Zone 5' at the same location as Zone T. As is shown in Figure 23 there is a secondary LPP shown as a thinner dashed line through Zone R and Zone U. Although minimal confidence is associated with this interpretation that conductors are interpreted to be linked; this is further interpreted to be linked to a gully in site C which wasn't investigated.

5.1.6 Site B Interpretation

Integration of the results for site B are depicted as Figure 24; interpretations for this site incorporated the least confident traced LPP of the investigation. Minimal confidence is derived on the positioning of the ERI survey lines which detected the interpreted associated conductor on the edge of profiles ER7 and ER8. Traced LPP for site B is as follows: **Gully 3 → Zone F → Zone H → Zone J**. The connection between the conductors represented as the head cut of the gully and Zone F is interpreted with confidence; as the trace conforms to the local topography and conductivity values match the outlined targeted values. Past this further connection to Zone H and J are given minimal confidence depicted as thin dashed lines; it is inferred that the limits of LPP detection/interpretation for site B is Zone F (~50m uphill). Due to the minimal confidence in the model this LPP isn't labeled and further investigation into the site is required for a confident model to be generated.

FEM results represented as Figure 10 depicted similar findings to the ERI in that the limits of detection are ~50m. F4 confirms the location of the gully channel as distinct peaks in HC and PC while F5 supports the traced LPP from the head cut to Zone F as conductivity peaks shown as 'Conductive Zone 2'. F6 moderately supports the location of Zone F as 'Anomalous Zone 2'.

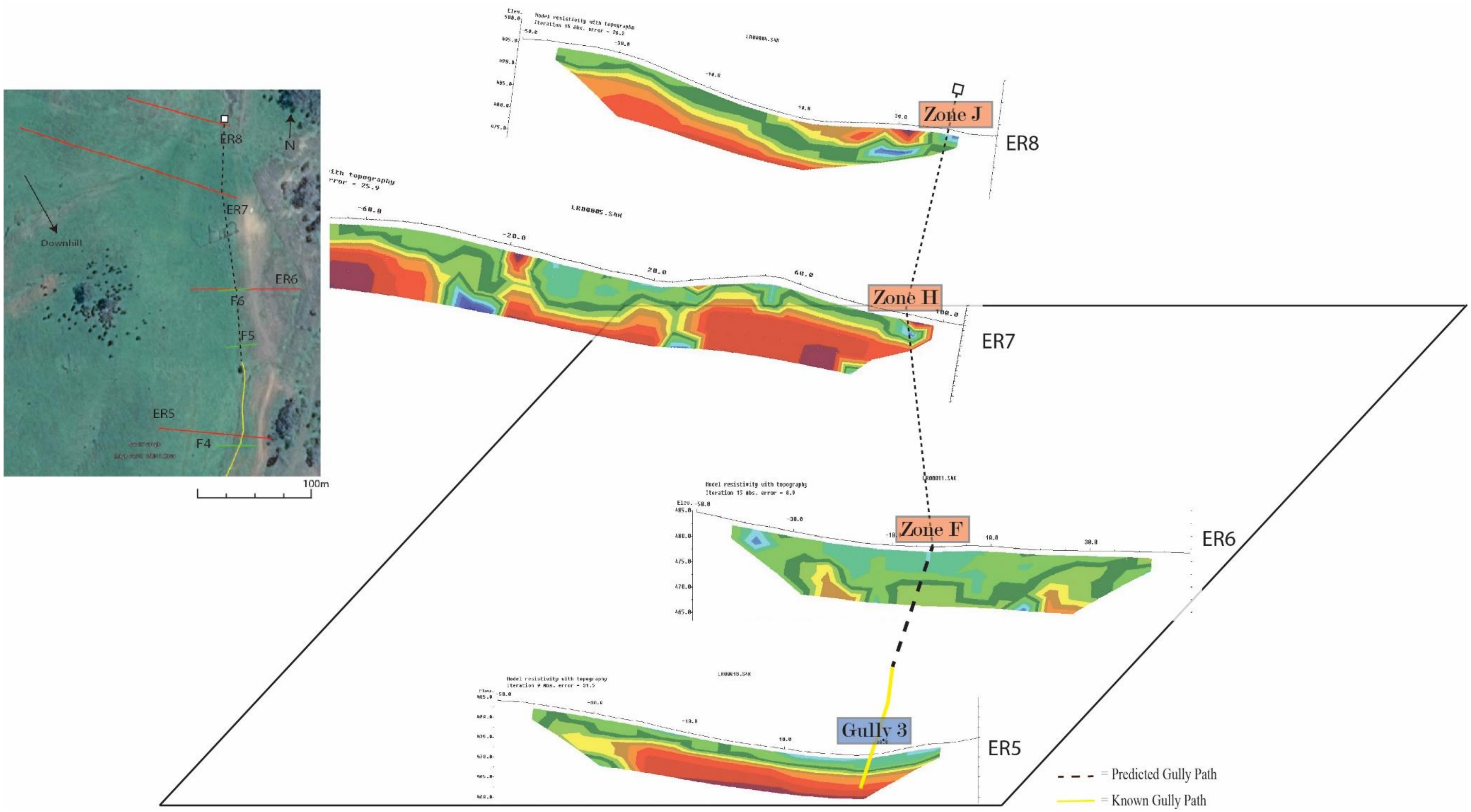

Figure 24. Integrated ERI results with an associated Google Earth image for site B; depicting the interpreted LPP shown as the black dashed line which intersects each profile through a shallow conductor.

5.2 Evaluation of Geophysical Investigation of LPP

As stated previously ERI and FEM have been successfully implemented in environmental soil studies and hydrological surveys. It was hypothesised initially that both ERI and FEM would be successful in detecting shallow conductors; it was found that ERI was effective in detecting small scale relative variations in the soil characteristics such as the targeted conductors (Corwin and Lesch, 2005b, Robinson et al., 2008). FEM was only minimally effective in detecting spikes in conductivity representative of targeted zones, it supported interpretations based on ERI but couldn't be implemented as a singular technique. It is suggested that if finances and time-constraints agree that FEM be implemented into ERI investigations of LPP as supplementary information to support traces. ERI is a required technique and can be implemented as a singular method if appropriate spacings are determined; as it is illustrated through the results that ERI was successful in detecting near-surface conductive anomalies uphill from existing gully head cuts.

Interpretations that targeted shallow conductors within a 1-40 Ωm range defined as 'Zones' represent areas of higher moisture content is supported through previous near-surface geophysical studies. This range was determined based on the measurement of the resistivity of background soil depicted through Figure 19; it illustrated that shale soils with no association to features exhibited ~100-500 Ωm. Based on this profile relative differences between anomalous shallow conductors and normal soil can be determined. Numerous studies identified conductive anomalies within similar ranges to the identified targeted conductors in this investigation and were also interpreted as water and/or saturated material, these studies include; Schmutz et al. (2009), Carrazza and Helene (2016) and Lazzari et al. (2010).

The investigation conducted by Schmutz et al. (2009) involved detecting internal structures of earthflows using the same techniques (ERI & FEM) proposed in this study. Results of both techniques depicted that zones of lower resistivity relative to surrounding areas of higher resistivity were indicative of earthflows. Other observations that were made based on the results was that near-surface conductive anomalies of 0-30 Ωm were related to areas of higher saturation relative to surrounding material. Interpretations of these geophysical results were all based on relative differences in conductivity and resistivity values within the measured profiles.

Carrazza and Helene (2016) and Lazzari et al. (2010) both implemented ERI in the investigation of cavities/voids within the subsurface associated to structural failure of large zones of soil. Findings from both these investigations found that high resistivity (>1000 Ωm) zones were representative of cavities/voids, a secondary finding was that highly conductive (0-300) zones were interpreted as highly saturated material relative to the background soil resistivity (300-500 Ωm).

Information and results presented in these studies reinforces the concept that these near-surface conductors are representative of saturated material (Carrazza and Helene, 2016), which can be associated to zones of higher water infiltration generated by variations in topography. It can be further hypothesised that these conductors are linked as a LPP for overland and shallow groundwater flows; this is depicted by the differences in resistivity seen between identified zones and measured background material. Links between conductors that are seen as the traced dashed lines generally follow the large scale topography of the area and mirror existing well-developed gullies enhancing the confidence in the interpreted line. Conceptually an LPP is supported through literature as a 'Soil Piping Phenomenon' which is described as horizontal or vertical pathways that concentrate flows due to variations in topography and soil characteristics (Vanmaercke et al., 2016). To infer that these obvious conductive anomalies are linked is reasonable and justified, similar associations are made by Lazzari et al. (2010) which links subsurface zones of saturated soil/rock between ERI profiles.

To take this one step further is to then propose that tracing LPP as linkages between these anomalous conductors is illustrative of future GHR, the pathway of future gully erosion. This concept that a LPP is a potential predictive model is based on the before mentioned 'Soil Piping Phenomenon' and the cohesive behaviour of water to channel. Therefore, it reasonable to assume that the modelled LPP are indicative of future head cut retreat as it represents the channel of water flow for near-surface and overland flows which are identified as the main driver for GHR (Beavis, 2000, Vanmaercke et al., 2016). Based on the findings in this investigation it is then plausible to implement the detection of LPP as a predictive model for gully erosion for the Tamworth area. Although the notion that LPP can be used as a proxy for GHR theory there is no measured evidence due to associated challenges with time, this being gully erosion occurring over years. It is suggested that continued monitoring of the identified gullies and traced LPP be implemented to evaluate the potential to predict GHR using ERI.

5.3 Applicability of Proposed Method

Based on the findings in this investigation the proposed field method is applicable as a gully assessment technique for the prediction of future pathways and locating critical points associated with continuous gullies. The initial methodology implemented in this study has since been updated according to the outcomes of the results section; an improved method of analysis is proposed. To outline the benefits of the proposed method it is compared to existing methods which are employed to assess the geomorphology, detrimental effects and overall evaluation of gullies with respect to agriculture and infrastructure, these include; Repeat Photography (observations), LiDAR/modelling and photogrammetry.

5.3.1 Proposed Field Method

Although the field method was effective in achieving the aim to detect shallow conductors the efficiency can be improved and cost minimised through optimisation; adjustments to the proposed method are suggested. A preliminary investigation would involve a visual assessment and point GPS of existing gullies within the site. Prioritisation of gullies is dependent on the location, development stage and associated risks; this will determine the targeted gullies if there are minimal funds for investigation (Wu and Cheng, 2005). Primary investigation would involve ERI conducted over the assumed head cut and then uphill from this position in 20-30m intervals up to ~70m distance from first survey; additional surveys in between intervals may be required after processing of data depending on the complexity of the area. FEM isn't required for the detection of LPP or critical points but can be used to support/inform the traced pathways of LPP between ERI lines as well as confirm locations of critical points. Data collected is then inputted into GIS software for traces to be interpreted and management strategies to be developed.

5.3.2 Current Field Methods

Repeat Photography:

Repeat Photography is a visual assessment of gullies in that at defined intervals of time (Months – Years) photos of identified gullies are taken to assess the rate and extent of gully extension; sediment removal rate and GHR (Frankl et al., 2012). It involves minimal costs and labour although it has minimal potential for informing management practices as it is purely a visual assessment of extension relative to other methods in which parameters can be measured and models generated. This type of assessment is usually combined with another form of assessment as supplementary information

.

LiDAR/Modelling:

LiDAR is employed in gully studies as a ground based assessment which involves measuring of high resolution topographic data and exceeds at detecting landforms such as gullies (Preti et al., 2013). As a field assessment of gullies LiDAR is relatively expensive and is limited in the amount of data which is collected, normally confined to small areas so large-scale investigations would be ineffective in terms of time and cost. Although the quality of data is high in that it is used to generate digital terrain maps and statistical models which are used in the prediction of future erosion associated to gullies (Eustace et al., 2011). Interpreted predictions based on the models are generally associated with modest results/confidence.

Photogrammetry:

Photogrammetry involves a series of paired photos which are stitched together to generate a high spatial resolution 3-Dimensional dataset to model and visualise small scale surface erosion. As a field assessment for gully erosion it is extremely effective in modelling the status of individual gullies but is extremely expensive and labour intensive due to required manpower, equipment, construction costs and software/processing (Wells et al., 2016). Due to the high-quality data produced by photogrammetry it is a plausible technique to implement when large funds are dedicated to the investigation, e.g. situations in which large firms are involved.

5.3.3 Comparison of Field Methods

Geophysics is known to be a cost effective investigative tool; in the case of ERI on gullies it can inexpensive relative to other techniques and provide valuable insight to future directions of existing gullies (Corwin and Lesch, 2005b). Minimal costs and labour are associated with photography but minimal benefits are gained from this form of assessment as it is a real-time visual assessment; only observing the retreat rather than assessing current conditions of the channel and GHR. Photogrammetry is extremely expensive but incorporates high quality data with potential for interpretations; this method would be impractical for multiple gully or large-scale investigations (Wells et al., 2016). LiDAR is moderately expensive and provides information of the geomorphology and elevation of critical points of the gully allowing for overall assessments of current conditions to be interpreted (Preti et al., 2013). It is recommended that an integration between LiDAR and ERI analysis of gullies is implemented for a complete understanding of current and future parameters. Although this is a costly procedure for infrastructure related studies it is necessary; for farmland based investigations potential smaller ERI surveys could be implemented for targeted management ~10m uphill from gully location.

5.4 Relevance of Research

Based on the results presented in this investigation the ability for electrical geophysics to be implemented as a form of gully assessment in the prediction of GHR and detection of critical points has been illustrated. Although it cannot assess the environmental effects of gullies (sediment loading etc.) it can be used to measure and locate critical points on continuous or discontinuous gullies to assist in management planning (Nyssen et al., 2004). Integrated geophysical and environmental assessments of continuous gullies lead to a greater understanding of current detrimental effects and prediction of GHR. Based on the results from these assessments **critical locations** of gullies are determined allowing for appropriate management solutions to be developed and implemented ensuring cost effective and successful remediation/prevention (Bourman and James, 1995, Poesen et al., 2003).

5.4.1 Critical Locations of Continuous Gullies

Management of gully erosion incorporates the assessment of the current effects on the environmental and urban features; based on the information produced in these assessment the appropriate management solutions can be determined and employed. Implementation of these solutions requires careful planning and consideration, usually the **critical points** of the gully are defined and then located as focal points for remediation strategies. These critical points are defined in this investigation as crucial locations for gully extension rather than all erosional features associated with gullies (widening of the channel and the mouth of the gully). Both continuous and discontinuous gullies incorporate a head cut as a critical point in which the channel will extend uphill; which is associated to the predicted LPP. Although discontinuous gullies being disconnected landforms incorporate a secondary critical point as an alluvial fan which is indicative of the downhill extension (Heede, 1982, Nyssen et al., 2004). Through the detection and outlining of these critical points for either gully type management strategies, such as check dams, can be implemented with locational information for targeted remediation. Targeting these critical points increases the effectiveness and chance of success for management and remediation of gully systems (Nyssen et al., 2004).

As mentioned previously this investigation focused on continuous gullies which generally extend downhill to a larger channel; this is the case as the studied gullies were connected to a main channel to the west. It was found the measurable points for continuous gullies incorporates the obvious features as the channel and head cut as well as the non-obvious LPP feature detected through geophysics uphill from the gully (Beavis, 2000, Le Roux and Sumner, 2012). These identifiable features represent the critical points of continuous gullies for which information is required to develop management strategies [Corwin, D & Lesch, S. 2005 [2]]. Through accurate detection of these features;

particularly the shallow conductors of an LPP, prediction pathways of GHR can be interpreted and traced leading to targeted management decisions. Based on the knowledge that non-obvious features associated with gully extension can be detected it is assumed that the same technique proposed in this study could be utilised to predict downhill extension of discontinuous gullies. It is suggested that a separate geophysical investigation into the potential prediction of downhill gully retreat for discontinuous gullies be conducted.

5.4.2 Integrated Assessment & Targeted Management

This study has proposed a potential field method for the prediction of GHR through the detection of a newly suggested critical point referred to as an LPP. Although through geophysical investigations of these only prediction models are obtained, this suggests that an integration with an environmental assessment method is required. Through integration of differing assessment techniques, a complete and holistic dataset of gullies can be developed allowing for maximum effectiveness in targeted management strategies. It is suggested that for the studied continuous gullies and other networks with similar landforms that a combination of **ERI and LiDAR** be implemented due to the high quality and amount of the information gathered relative to the labour/cost required. Through these assessments an informed evaluation of specific gullies can be determined allowing for moderate to intense remediation depending on the estimated priority. By informing management decisions of critical locations, predicted pathways and prioritisation the effectiveness of gully remediation and prevention methods implemented will be improved significantly (Le Roux and Sumner, 2012).

Chapter 6: Conclusions

Based on the literature current predictive models for GHR are ineffective or developed with minimal confidence which leads inappropriate management strategies (Valentin et al., 2005). This lack of predictive tools for head cut retreat is due to the fact these models are based purely on visual assessments through time or measurements of select surface parameters. Currently the focus is direct remediation of visible features through physical alteration of the channel or construction of concrete check dams; preventative measures are reliant on prediction models which as stated earlier are currently ineffective (Le Roux and Sumner, 2012, Nyssen et al., 2004). There is an ever-growing necessity for prevention rather than remediation which leads to the fact that effective predictive models are required (Clothier et al., 2007). This study has proposed a method of GHR prediction through the detection of shallow conductors which are representative as a Longitudinal preferential pathways act as a proxy for the pathway of uphill gully retreat. Based on the findings and aims of this investigation the following conclusions have been made:

(1) Electrical Resistivity Imaging was successful at proving and detecting the existence of shallow conductors uphill of gully head cuts representative as the proposed LPP concept for continuous gullies. It is then plausible for geophysical investigations to be implemented as a potential predictive method for GHR. Limit of accurate detection of LPP conductors uphill from head cuts is ~70m; this can be extended if spacing between surveys is reduced which leads to increased costs for minimal benefits.

(2) Inclusion of Longitudinal preferential pathways as a measurable and significant critical point in gully assessments along with the commonly accepted critical points such as; Head cut, Channel, Mouth of the Channel (Continuous) and the Alluvial fan (Discontinuous).

(3) Frequency Electromagnetics is unable to detect relatively subtle features such as LPP as it relies on bulk conductivity variations. In terms of LPP detection it is plausible to implement as supplementary information to assist in interpretation; although the limits of detection were determined to be 0-15m uphill from the head cut. There is scope for FEM to be implemented for detection of traditional critical points as the head cut was often outlined by conductivity peaks.

(4) It is inferred that identified conductive anomalies with associated traces through them are linked as a Lateral Preferential Pathway; it seems unlikely that these connections are merely a coincidence due to the uncanny conformity to the slope and similar style to existing gullies exhibited. Based on this these pathways can be inferred with high confidence as the pathway for GHR.

Future Directions

Through this investigation a new method of gully assessment has been developed using electrical geophysics as a predictive tool. Beyond this study there is substantial scope for further analysis of the identified gullies as well as posing new research questions generated by the results; potential future directions derived from this investigation include:

- Continued monitoring of identified gullies in the next few months/years to measure the correlation between the predicted Gully Head cut Retreat pathway shown as the traced LPP and the actual erosional pathway

- Additional ERI surveys conducted for LPP models with minimal confidence to improve the overall interpretation of the GHR pathway

- Investigations into critical locations of discontinuous gullies; focusing on the alluvial fan as a predictive tool for downhill gully extension

- Investigations into differing gully types relative to the identified gullies in this study to understand the potential for global implementation (Steeper slopes, differing geological background and potentially gullies threatening infrastructure)

References

AITCHISON, J. C., FLOOD, P. G. & SPILLER, F. C. P. 1992. Tectonic setting and paleoenvironment of terranes in the southern New England orogen, eastern Australia as constrained by radiolarian biostratigraphy. *Palaeogeography, Palaeoclimatology, Palaeoecology,* 94**,** 31-54.

BEAVIS, S. G. 2000. Structural controls on the orientation of erosion gullies in mid-western New South Wales, Australia. *Geomorphology,* 33**,** 59-72.

BOURMAN, B. & JAMES, K. 1995. Gully evolution and management: a case study of the Sellicks Creek Drainage Basin. *South Australian Geographical Journal,* 94**,** 81-105.

CARRAZZA, L. P. M., CESAR AUGUSTO & HELENE, L. P. I. 2016. Gully cavity identification through electrical resistivity tomography. *Brazillian Journal of Geophysics,* 34**,** Draft.

CHAPPELL, B. W. 1961. *The stratigraphy and structural geology of the Manilla-Moore creek district, N. S. W.* Sydney, N.S.W.: Sydney, N.S.W., Australia: Royal Society of New South Wales.

CHAPPELL, B. W. 1968. Volcanic greywackes from the upper Devonian Baldwin Formation, Tamworth-Barraba District, New South Wales. *Journal of the Geological Society of Australia,* 15**,** 87-102.

CLOTHIER, B. E., GREEN, S. R. & DEURER, M. 2007. Preferential flow and transport in soil: progress and prognosis. *European Journal of Soil Science,* 59**,** 2-13.

COLLISON, A. J. C. 2001. The cycle of instability: stress release and fissure flow as controls on gully head retreat. *Hydrological Processes,* 15**,** 3-12.

CORWIN, D. L. & LESCH, S. M. 2005a. Apparent soil electrical conductivity measurements in agriculture. *Computers and Electronics in Agriculture,* 46**,** 11-43.

CORWIN, D. L. & LESCH, S. M. 2005b. Characterizing soil spatial variability with apparent soil electrical conductivity. *Computers and Electronics in Agriculture*, 46**,** 103-133.

DOTTERWEICH, M., STANKOVIANSKY, M., MINÁR, J., KOCO, Š. & PAPČO, P. 2013. Human induced soil erosion and gully system development in the Late Holocene and future perspectives on landscape evolution: The Myjava Hill Land, Slovakia. *Geomorphology,* 201**,** 227-245.

EUSTACE, A. H., PRINGLE, M. J., DENHAM, R. J. & LARK, R. M. 2011. A risk map for gully locations in central Queensland, Australia. *European Journal of Soil Science,* 62**,** 431-441.

FRANKL, A., POESEN, J., DECKERS, J., HAILE, M. & NYSSEN, J. 2012. Gully head retreat rates in the semi-arid highlands of Northern Ethiopia. *Geomorphology,* 173-174**,** 185-195.

HEEDE, B. 1982. Gully control: Determining treatment priorities for gullies in a network. *An International Journal for Decision Makers, Scientists and Environmental Auditors,* 6**,** 441-451.

LAZZARI, M., LOPERTE, A. & PERRONE, A. 2010. Near surface geophysics techniques and geomorphological approach to reconstruct the hazard cave map in historical and urban areas. *Advances in Geosciences,* 24**,** 35-44.

LE ROUX, J. J. & SUMNER, P. D. 2012. Factors controlling gully development: Comparing continuous and discontinuous gullies. *Land Degradation & Development,* 23**,** 440-449.

MELLIGER, J. J. & NIEMANN, J. D. 2010. Effects of gullies on space–time patterns of soil moisture in a semiarid grassland. *Journal of Hydrology,* 389**,** 289-300.

NAZARI SAMANI, A., AHMADI, H., MOHAMMADI, A., GHODDOUSI, J., SALAJEGHEH, A., BOGGS, G. & PISHYAR, R. 2009. Factors Controlling Gully Advancement and Models Evaluation (Hableh Rood Basin, Iran). *Water Resources Management,* 24**,** 1531-1549.

NYSSEN, J., VEYRET-PICOT, M., POESEN, J., MOEYERSONS, J., HAILE, M., DECKERS, J. & GOVERS, G. 2004. The effectiveness of loose rock check dams for gully control in Tigray, northern Ethiopia. *Soil Use and Management,* 20**,** 55-64.

PERROY, R. L., BOOKHAGEN, B., ASNER, G. P. & CHADWICK, O. A. 2010. Comparison of gully erosion estimates using airborne and ground-based LiDAR on Santa Cruz Island, California. *Geomorphology,* 118**,** 288-300.

POESEN, J., NACHTERGAELE, J., VERSTRAETEN, G. & VALENTIN, C. 2003. Gully erosion and environmental change: importance and research needs. *Catena,* 50**,** 91-133.

POHLER, S. 1998. Devonian carbonate buildup facies in an intra-oceanic island arc (Tamworth Belt, New South-Wales, Australia). *International Journal of Paleontology, Sedimentology and Geology,* 39**,** 1-34.

PRETI, F., TAROLLI, P., DANI, A., CALLIGARO, S. & PROSDOCIMI, M. 2013. LiDAR derived high resolution topography: The next challenge for the analysis of terraces stability and vineyard soil erosion. *Journal of Agricultural Engineering,* 44**,** 85-89.

ROBINSON, D. A., BINLEY, A., CROOK, N., DAY-LEWIS, F. D., FERRÉ, T. P. A., GRAUCH, V. J. S., KNIGHT, R., KNOLL, M., LAKSHMI, V., MILLER, R., NYQUIST, J., PELLERIN, L., SINGHA, K. & SLATER, L. 2008. Advancing process-based watershed hydrological research using near-surface geophysics: a vision for, and review of, electrical and magnetic geophysical methods. *Hydrological Processes,* 22**,** 3604-3635.

SAMANI, A. N., CHEN, Q., KHALIGHI, S., WASSON, R. J. & RAHDARI, M. R. 2016. Assessment of land use impact on hydraulic threshold conditions for gully head cut initiation. *Hydrology and Earth System Sciences,* 20**,** 3005-3012.

SCHMUTZ, M., GUÉRIN, R., ANDRIEUX, P. & MAQUAIRE, O. 2009. Determination of the 3D structure of an earthflow by geophysical methods. *Journal of Applied Geophysics,* 68**,** 500-507.

SHIT, P. K. & MAITI, R. K. 2012. Mechanism of Gully-Head Retreat - A Study at Ganganir Danga, Paschim Medinipur, West Bengal. *Ethiopian Journal of Environmental Studies and Management,* 5.

SIDORCHUK, A. 1999. Dynamic and static models of gully erosion. *Catena,* 37**,** 401-414.

STAVI, I., PEREVOLOTSKY, A. & AVNI, Y. 2010. Effects of gully formation and headcut retreat on primary production in an arid rangeland: Natural desertification in action. *Journal of Arid Environments,* 74**,** 221-228.

STEIN, O. R. & LATRAY, D. A. 2002. Experiments and modeling of head cut migration in stratified soils. *Water Resources Research,* 38**,** 20-1-20-12.

VALENTIN, C., POESEN, J. & LI, Y. 2005. Gully erosion: Impacts, factors and control. *Catena,* 63**,** 132-153.

VANMAERCKE, M., POESEN, J., VAN MELE, B., DEMUZERE, M., BRUYNSEELS, A., GOLOSOV, V., BEZERRA, J. F. R., BOLYSOV, S., DVINSKIH, A., FRANKL, A., FUSEINA, Y., GUERRA, A. J. T., HAREGEWEYN, N., IONITA, I., MAKANZU IMWANGANA, F., MOEYERSONS, J., MOSHE, I., NAZARI SAMANI, A., NIACSU, L.,

NYSSEN, J., OTSUKI, Y., RADOANE, M., RYSIN, I., RYZHOV, Y. V. & YERMOLAEV, O. 2016. How fast do gully headcuts retreat? *Earth-Science Reviews,* 154**,** 336-355.

WELLS, R. R., ALONSO, C. V. & BENNETT, S. J. 2009. Morphodynamics of Headcut Development and Soil Erosion in Upland Concentrated Flows. *Soil Science Society of America Journal,* 73**,** 521.

WELLS, R. R., MOMM, H. G., BENNETT, S. J., GESCH, K. R., DABNEY, S. M., CRUSE, R. & WILSON, G. V. 2016. A measurement method for rill and ephemeral gully erosion assessments. *Soil Science Society of America Journal,* 80**,** 203-214.

WILKINSON, S. N., DOUGALL, C., KINSEY-HENDERSON, A. E., SEARLE, R. D., ELLIS, R. J. & BARTLEY, R. 2014. Development of a time-stepping sediment budget model for assessing land use impacts in large river basins. *Sci Total Environ,* 468-469**,** 1210-24.

WU, Y. & CHENG, H. 2005. Monitoring of gully erosion on the Loess Plateau of China using a global positioning system. *Catena,* 63**,** 154-166.

ZHOU, Q. Y., SHIMADA, J. & SATO, A. 2001. Three-dimensional spatial and temporal monitoring of soil water content using electrical resistivity tomography. *Water Resources Research,* 37**,** 273-285.

Appendix A – GPS Coordinate Table

Table 1. GPS coordinates of all start and ends of geophysical surveys as well as lengths and rough GPS locations of surveyed gullies for each site. WGS 1984 – UTM 56J

Site	Line/Feature Number	Northern/Start Point		Southern/End Point		Length (m)
		South	East	South	East	
A	ER1	6561954.1	301201.77	6561873.26	301247.52	100
	ER2	6561987.55	301271.86	6561897.25	301312.29	100
	ER3	6561994.78	301307.76	6561897.86	301336.43	100
	ER4	6562118.14	301363.31	6561913.83	301361.51	200
	F1	6561923.93	301214.78	6561882.03	301240.48	50
	F2	6561936.2	301249.59	6561908.99	301265.18	30
	F3	6561951.14	301269.09	6561921.71	301296.29	40
	Gully 1	6561923.23	301260.98	6561906.44	301218.11	~
B	ER5	6561011.94	301966.37	6561005.08	302068.09	100
	ER6	6561122.2	301992.96	6561123.71	302092.96	100
	ER7	6561257.48	301834.89	6561197.06	302037.58	200
	ER8	6561281.4	301933.01	6561255.25	302030.53	100
	F4	6560998.86	302014.5	6561000.05	302053.21	30
	F5	6561074.5	302023.54	6561079.34	302056.2	30
	F6	6561120.6	302018.46	6561122.8	302049.74	30
	Gully 3	6561064.65	302039.01	6560965.2	302023.7	~
C	ER9	6561729.89	301218.73	6561556.73	301316.81	200
	ER10	6561726.57	301250.75	6561644.09	301300.89	100
	ER11	6561709.59	301314.68	6561627.35	301363.07	100
	ER12	6561749.33	301388.15	6561655.77	301424.88	100
	F7	6561730.14	301220.56	6561642.84	301271.21	100
	F8	6561727.76	301249.93	6561643.85	301306.79	100
	F9	6561660.68	301317.88	6561633.78	301332.09	30
	F10	6561675.21	301331.4	6561644.79	301345.13	30
	Gully (K1)	6561651.83	301256.12	6561616.11	301217.46	~
	Gully 5	6561642.55	301362.28	6561607.09	301298	~
D	ER13	6561855.02	301331.17	6561756.4	301348.42	100
	ER14	6561878.02	301365.81	6561680.65	301366.09	200
	F11	6561878.02	301365.81	6561680.65	301366.09	200
	Gully	6561804.65	301311.47	6561744.69	301240.9	~
E	ER15	6561204.83	301777.01	6561211.51	301882.7	100
	ER7	6561257.48	301834.89	6561197.06	302037.58	200
	Gully	6561193.55	301832.38	6561178.8	301831.54	~